Exploring the role of Mon1 in *Drosophila* ovary development

INDIAN INSTITUTE OF SCIENCE EDUCATION AND RESEARCH, PUNE

In partial fulfilment of the

for the award of the degree of 5 years

BS-MS dual degree

By

Neena Dhiman

20121093

Under the guidance of

Dr. Anuradha Ratnaparkhi

Developmental Biology Group

ARI, PUNE

Certificate

This is to certify that this dissertation entitled "**Exploring the role of Mon1 in *Drosophila* ovary development**" towards the partial fulfilment of the BS-MS dual degree programme at the Indian Institute of Science Education and Research, Pune represents work carried out by "Neena Dhiman at IISER, Pune" under the supervision of "Dr. Anuradha Ratnaparkhi, Developmental Biology Group, Agharkar Research Institute, Pune" during the academic year 2016-2017

Date: 20-03-2017

Signature of the Supervisor

Signature of the candidate

Neena Dhiman

20121093

Declaration

This is to certify that work presented in this project entitled "**Exploring the role of Mon1 in *Drosophila* ovary development**" Submitted by **Neena Dhiman, Reg. No. 20121093** to **Indian Institute of Science Education and Research, Pune** in partial fulfillment of the requirement for the award of the degree of BS-MS dual degree. It has been successfully complete and comprises the results of independent and original work carried out by me under the supervision of **Dr. Anuradha Ratnaparkhi.** The full work or any part of it reported here has not been submitted for the award of any degree.

Date: 20-03.2017

Signature of the Supervisor

Signature of the candidate
Neena Dhiman
20121093

ACKNOWLEDGEMENT

I would like to express my gratitude to my guide Dr. Anuradha Ratnaparkhi, ARI Pune for all her unconditional support and patience guidance. I have learned and gained very much from her; for that, I am very grateful. Without her guidance and persistent help, this project would not have been possible.

I would like to express my gratitude to Dr.Girish Ratnaparkhi for providing me with an opportunity to work in his laboratory as well as granting me full freedom to use the facilities available.

I would like to thank Dr. Raghav Rajan, TAC member, for his critical comments throughout my project and Dr. Richa Rikhy for helpful discussions.

I would like to thank Dr. Senthil D. (GR Lab) who introduced me to the workplace as well as guided me through the crucial early stages of my project work.

I would thank my lab mates from both GR and AR labs: Prajna, Vallari, Bhagyashree, and Anagha. Special thanks to all the members of GR Lab, RR Lab and AR Lab for an immensely valuable learning experience that this has been and for adding the touch of fun to my time in the lab.

I would like to sincerely thank IISER, Pune for permitting me to take up my MS project.

Abstract

The involvement of the nervous system and the mechanisms regulating organ development and regeneration is a area that is gaining prominence. In the present study, we have tried to understand the molecular basis for sterility in *Dmon1* mutants. These mutants show extremely small ovaries with fewer ovarioles and egg chambers that fail to progress through the vitellogenic phase. We find that neuronal expression of *Dmon1* rescues the ovary phenotypes. More specifically, we find that expression in octopaminergic neurons is sufficient for the rescue. Using RNAi against *Dmon1*, we show that the phenotype is neuronal in origin and not ovarian suggesting that Mon1 regulates *Drosophila* ovary development in non-cell autonomous manner. To understand the mechanism of this regulation we have examined the role of insulin signaling in these mutants. We find that expression of some of the *dilps* is significantly reduced in $Dmon1^{\Delta 181}$ mutants (mutants carrying a deletion of the C-terminus) and feeding insulin to $Dmon1^{\Delta 181}$ flies results in the rescue of the ovary phenotypes and a mild improvement in life span. Our results suggest that *Dmon1* regulates ovary development by regulating the synthesis and/or secretion of insulin-like peptides in the brain.

Table of contents

1. Introduction……..……8

2. Materials and methods……15

3. Results……...21

3.1. Mon1 mutants are sterile and have reduced ovaries……..21

3.2. *Dmon1 mutant* egg chambers exhibit stalling and degeneration……...…24

3.3. *Orb* levels are down regulated in *Dmon1$^{\Delta 181}$ mutants*…….....27

3.4. *Dmon1$^{\Delta 181}$/ Dmon1$^{\Delta 181}$* mutant phenotype is rescued by expression of Mon1 in neurons…….……....29

3.5. Neuronal knock-down of Mon1 is sufficient to give ovary phenotype……33

3.6. Dilps are affected in *Dmon1$^{\Delta 181}$* mutant……..……36

3.7. Insulin feeding partially rescues the *Dmon1$^{\Delta 181}$* ovary phenotype……..……40

3.8. Protein purification for antibody generation…….....43

4. Discussion……..…..47

5. References……..…..50

List of Figures

Figure1: Organization of the *Drosophila* ovary. ……..…....9

Figure2: The endocytic pathway. ……..……...……11

Figure3: Role of Mon1 in endocytosis. ..…….……..….....12

Figure 3.1.1: *Dmon1* $^{\Delta 181}$ flies are small… ……..…….....21

Figure3.1.2: Characterization of the ovarian morphology in *Dmon1* mutants. ……....23

Figure3.2.1: *Dmon1* $^{\Delta 181}$ mutants have small ovarioles. ..……....24

Figure3.2.2: Pie charts showing the occurrence of the different stages of egg chambers in wildtype and *Dmon1* mutant ovarioles. ..……....25

Figure 3.2.3: *Dmon1* mutant ovarioles exhibit degeneration. ……..…26

Figure3.3.1: Expression of Orb is reduced in *Dmon1*$^{\Delta 181}$ mutants. ..……..….27

Figure3.3.2: Quantitative RT-PCR and Western blot to measure Orb levels in mutant ovaries. ……...…28

Figure 3.4.1: Neuronal expression of *Dmon1* rescues the ovary phenotype in *Dmon1*$^{\Delta 181}$ mutants. ..……..…….……30

Figure 3.4.2: Expression of *Dmon1* in octopaminergic neurons is sufficient to rescue ovary size and ovariole number in *Dmon1*$^{\Delta 181}$ mutants. …….31

Figure3.4.3: Expression of *Dmon1* in octopaminergic neurons rescues Orb levels and the stalling defects.……...32

Figure3.5.1: Neuronal knock-down of Mon1 reduces ovary size. ……..…....33

Figure3.5.2: Quantitation of ovary length in *Dmon1* RNAi animals……34

Figure3.5.3: Knock-down of *Dmon1* in ovarian germline does not alter ovary size. ……35

Figure3.6.1: Expression of different *dilps* in $Dmon1^{\Delta 181}$ mutant flies. ……38

Figure3.7.1: Insulin feeding leads to a significant rescue of the $Dmon1^{\Delta 181}$ ovary phenotype……..……..41

Figure3.8.1: DMon1 protein expression and purification. ……..…….....44

Figure3.8.1: Troubleshooting to increase the yield of purified, cleaved Mon1. ….....46

List of tables

Table3.1.1: Lethality and fertility observed in different allelic mutants of *Dmon1*.....22

1. Introduction

The nervous system is one of the most complex organ systems that controls all motor and sensory functions in the body. In recent years, the role of the nervous system in regulating development and/or regeneration of organs is becoming evident. In animals like tadpole or echinoderms, it has been known that regeneration of limbs is dependent on the presence of a nervous system (Kumar and Brockes., 2012). Recent studies have shown that during salivary gland development, parasympathetic innervation plays an important role in maintaining the epithelial progenitor cells in an undifferentiated state essential for regeneration (Hoffman *et al*., 2013). In *Drosophila* too, there have been reports on the role of the nervous system in regulating growth and development of organ systems. For example, homing and survival of haematopoetic cells is shown to be dependent on the peripheral nervous system. Ablation of subsets of these neurons leads to decrease in the number of haemocytes (Makhijani *et al*., 2011). Inputs from the peripheral nervous system have also been shown to regulate airway/tracheal development (Bower et al., 2014). However, the extent to which the nervous system might be involved in the development of an organ needs to be explored.

Drosophila ovarian system

Drosophila adult females has two ovaries, each made up of 16-20 tube-like structures called ovarioles which are functional units of the ovary. Each ovariole has a string of six to eight sequentially developing egg chambers. At the anterior tip of each ovariole, is the germarium which contains 2-3 germline stem cells (GSC) surrounded by terminal filament cells and cap cells to provide a niche or microenvironment to GSC. Each GSC typically undergoes asymmetric division producing one daughter germline stem cell and cytoblast. The newly formed cystoblast undergoes four incomplete mitotic division to form 16 interconnected cyst cells. Out of the 16 cells, one develops into the future oocyte, and the remaining 15 form the nurse cells which synthesize RNA, proteins, and organelles for the oocyte. The future oocyte is distinguished from the other cells due to the accumulation of transcripts of genes such like *orb*, *cup*, *BicD* and *Egl*. As the germline cyst cell progresses through germarium, the surrounding layer of somatic follicle cells starts forming the egg chambers in the region 2b of the

germarium. Each egg chamber then begins to move out of the germarium. Once the encapsulation of the cyst is over as shown in 3a region of germarium (Figure 1), it is pinched off from the germarium to form an egg chamber. These egg chambers undergo 14 defined stages of maturation. All the egg chambers are connected to each other by short stalk cells. Till stage 8, the size of the nurse cells and oocyte are similar; after that, the oocyte begins to increase in size significantly. They form a mature oocyte as the egg chamber proceeds towards the posterior end of the ovariole. At the end of stage 14, the egg passes through the lateral oviduct further enters into common oviduct and exits via the uterus (Buszczak *et al.,*2011).

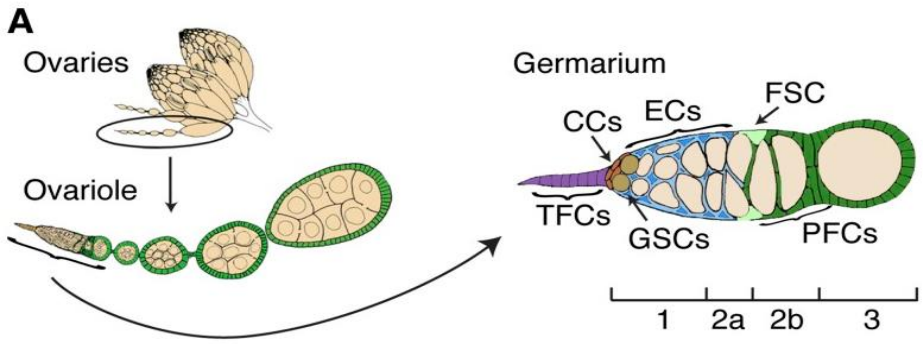

Huang *et al.* ,2014

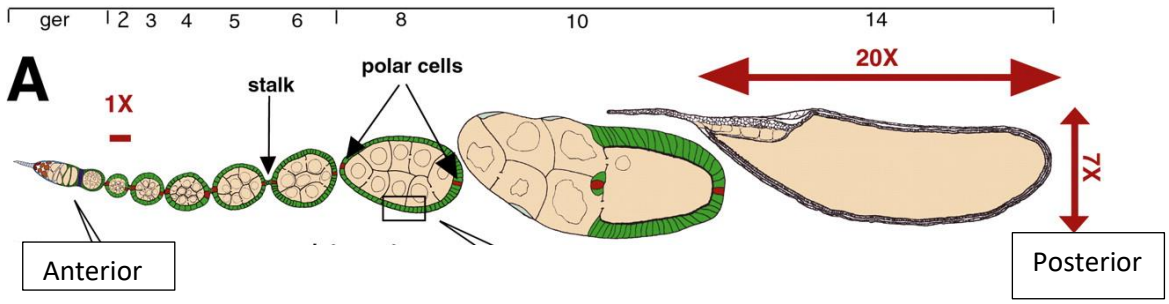

Horacio M. Frydman, and Allan C. Spradling Development 2001;128:3209-3220

Figure1: Organization of the *Drosophila* ovary.

An adult female contains two ovarioles; each ovary is made up of ovarioles which are developing egg chambers which are connected by short stalk cells. Germarium is located at the anterior end of the ovariole contains germ stem cells (GSC) surrounded by terminal filament cell(TFCs) and Cap cells(CCs) provide a microenvironment for the maintenance of the GSC. The germline cells divide asymmetrically to form the 16-cell cyst which when enclosed by an inner sheath of follicle cells to form an egg chamber. At the posterior end of the ovariole is a later stage egg chamber which has the developing oocyte.

The growth of the egg chamber can be broadly divided into two phases: the previtellogenic and vitellogenic phase. The vitellogenic phase is defined by the exponential growth of the oocyte. During this phase, yolk formation takes place in the oocyte. The transition from pre-vitellogenic to vitellogenic phase is under tight regulation by hormones and nutrition. The juvenile hormone (JH) is required for yolk formation and necessary for the vitellogenic process. This phase also involves extensive endocytosis by the oocyte. Nutritional status also plays an important role in the regulation of vitellogenesis. Signaling by insulin-like peptides links nutritional status to growth. There are 8 insulin-like peptides in *Drosophila*. Three of these, namely Dilp 2, 3 and 5 are produced by a set of neurons in the brain called as insulin producing cells or IPCs. These peptides are released into circulation through the axon terminals of the IPCs at the corpora cardiaca- a neurohemal organ (Brogiolo et al., 2001; Cao and Brown, 2001; Ikeya et al., 2002). Loss of insulin signaling affects oogenesis. Loss of the insulin substrate protein Chico leads to a reduction in the size of the ovary, inability of the egg chambers to enter the vitellogenic stages and sterility. (Richard *et al*., 2005; Barbosa and Spradling *et al.*, 2001)

Mechanisms that regulate insulin secretion are not well understood. Studies have shown that IPCs are likely to be under neuronal regulation: Short neuropeptide F (sNPF) and octopamine appear to stimulate IPC and insulin signaling while GABA is inhibitory (Lee *et al.*, 2008; Crocker *et al*., 2010; Enell *et al*., 2010; Luo *et al*., 2014). Insulin signaling affects a wide variety of developmental processes in an organism. Each process is likely to have its own regulatory circuit in the brain including a specific set of molecules involved in regulating signaling. The circuit and molecules involved in regulating egg chamber growth are not well understood.

Intracellular trafficking and secretion and Mon1:

Many molecules involved in regulating secretion also have overlapping roles in regulating endocytosis. For example, exosomes which arise from multivesicular bodies are marked by Rab7, which is also involved in trafficking of vesicles for fusion with the lysosome.

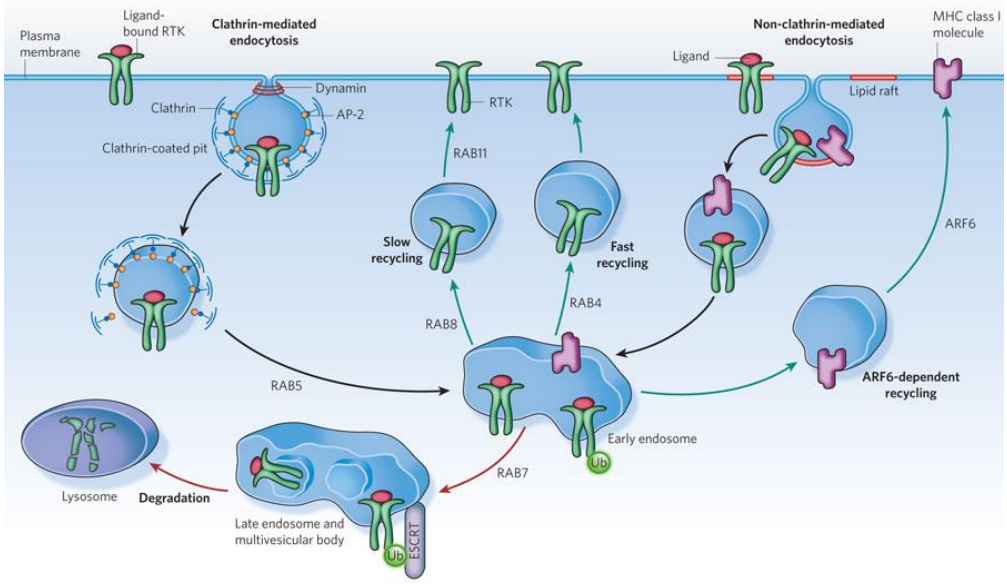

(*Scita and Fiore., 2010*)

Figure2: The endocytic pathway.

Clathrin-mediated endocytosis and non-clathrin mediated endocytosis. When ligand bound to receptor either of the ways, the vesicle internalized and fused with early endosome with the help of Rab5. From the early endosome, it can either follow recycling pathway or degradation pathway by recruiting different Rabs. Cargo can be slowly recycled (depends upon Rab8) or degraded pathway (depends upon Rab7) through late endosome and then to lysosomes.

Mon1 (Monensin sensitive 1) is a highly conserved endocytic protein with a longin domain (Ypt7 in yeast). In complex with CCZ1, it acts as a guanine nucleotide exchange factor (GEF) for the Rab7.Thus Mon1 is essential for the conversion of Rab5 positive early endosomes to Rab7 positive late endosomes (Poteryaev et al. 2010). Yeast, *Drosophila,* and *C.elegans* have one copy of Mon1 while humans have two related genes: Mon1a and Mon1b.

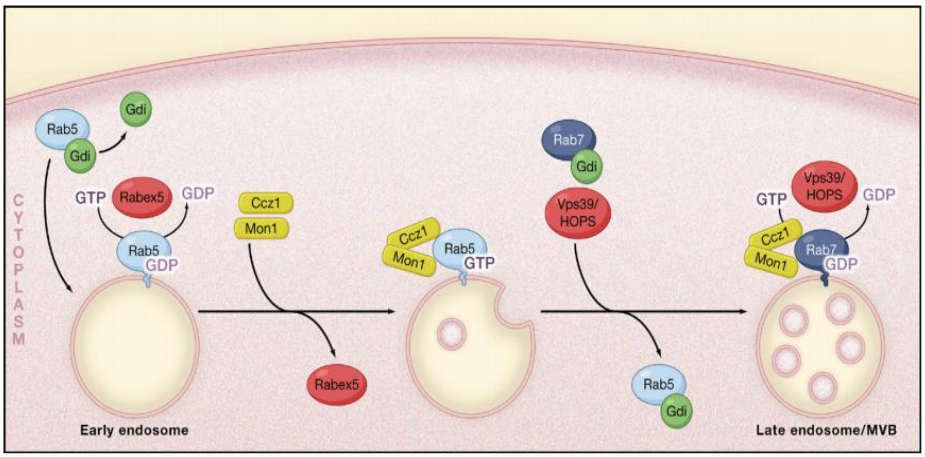

Margarita Cabrera and Christian Ungermann(2010). **Guiding endosomal maturation.** Cell 141

Figure3: Role of Mon1 in endocytosis.

In the endocytic pathway, Mon1 helps in conversion of early endosomes into late endosomes by recruiting Rab7 GTPase. Mon1 protein act as a switch that shut off the recruitment of Rab5 and further activates the Rab7 for its recruitment.

The conserved role of Mon1 across various organisms including plants is to recruit Rab7 to late endosomes. In yeast, mutations in Mon1 leads to defects in autophagy, pexophagy and degradative pathways which share protein machinery with the cytoplasm to the vacuole transport (CVT) pathway (Wang *et. al*,2002; Polupanov *et al.,*2011).

In *C.elegans* the Mon1-Ccz1 complex is necessary for removal of Rabex5 from the early endosomes which is required for maintaining Rab5 in its active form. It is also also required for recruitment of Rab7 to early endosomes thus converting them to late endosomes (Kinchen and Ravichandran., 2010). A similar role for Mon1 has been demonstrated in *Arabidopsis (*Cui *et al.* 2014). As in yeast and C.*elegans*, mutations in *Drosophila mon1* affects recruitment of Rab7 to endosomes and therefore the formation of late endosomes.

While the function of Mon1 is well characterized, its physiological relevance in different cellular contexts still needs to be addressed. It is also not clear if Mon1 has functions that are independent of CCZ1. In *Drosophila*, loss of Mon1-Ccz1-Rab7 in starved *Drosophila* fat cells accumulates autophagosomes due to impaired fusion with lysosomes. In this study, it was also shown that Rab5 is required for proper lysosomal function (Hegedus *et al.,*2016).

A recent study in Arabidopsis has shown that Mon1 mutants show a decrease in male fertility due to defects in both the tapetum and pollen coat formation (Cui *et al.,* 2017).

Origin of the project:

In the lab, mutations in *Dmon1* were generated using P-element mediated excision (Deivasigamani et al., 2015). *Dmon1*$^{\Delta 181}$ carries a deletion in the 3' region of the gene. A major area of interest in the lab is to study signalling at the neuromuscular junction in the context of synaptic development and neurodegeneration. Examination of the neuromuscular junction in *Dmon1*$^{\Delta 181}$ mutants showed the presence of high levels of glutamate receptors (GluRIIA) indicating that Mon1 is a negative regulator of GluRIIA. Homozygous *Dmon1*$^{\Delta 181}$ mutants seem to die throughout development and during eclosion. *Dmon1*$^{\Delta 181}$ mutant escapers are short lived with severe motor defects and are sterile. It was observed that neuronal rescue of lethality was also able to rescue the sterility defect in these mutants suggesting that the nervous system may play a role in regulating fertility in flies. How does the nervous system regulate fertility? As a first step towards understanding this process, we decided to examine the role of *Dmon1* in ovary development and how the nervous system may be involved in this process.

Hypothesis:

Mon1 regulates ovary development in non-cell autonomous manner.

Objectives and specific aims:

1. Conduct a detailed morphological and molecular characterization of the ovary defect in *Dmon1* mutants.
   a) Examine external morphology of the ovary in different allelic combinations of *Dmon1* in terms of size, ovariole number etc.
   b) Carry out immunohistochemistry on wildtype and mutant ovaries using antibodies against different markers like *Orb* to detect possible changes.

2. Determine the origin of the ovary phenotype by identifying possible autonomous and non-autonomous contributions of *Dmon1*.
   a) Using RNAi to determine tissue specific requirements of *Dmon1*.

3. Identify the underlying mechanism that gives rise to the ovary phenotype.

4. Examine localization of DMon1 in *Drosophila* through the generation of an antibody.

2. Materials and Methods:

1) Fly husbandry and stocks used:

All the stocks were reared on corn meal agar medium, *Dmon1*$^{\Delta 181}$ was generated in by excising the pUAST-Rab21::YFP insertion using standard genetic methods (Deivasigamani et al., 2015). The fly stocks, *Df(2L)9062,* C155-GAL4, tdc-2GAL4 were from Bloomington Stock stock centre, Indiana, USA; *Dmon1* RNAi line (CG11926) was from the VDRC stock centre; *UAS-mon1::HA* was a kind gift from T.Klein; pog1/CyoactGFP (kind gift from Stephen Kerridge, Mathew et al., 2009). All lines used in this study were generated using standard genetic methods. All crosses, except where mentioned were carried out at 25 degrees.

2) Immunohistostaining and Imaging:

For ovary morphology: Adult ovaries were dissected in chilled 1X PBS. Whole ovaries was imaged using Olympus Axio Zoom Stereoscope at 1x and subsequently processed using ImageJ.

For molecular characterization: Adult ovaries were dissected in chilled 1X PBS and fixed with 4% paraformaldehyde in 1X PBS with 0.3% Triton-X for 25 min at room temperature. They were washed 6 times with 1X PBS with 0.3% Triton-X for 15 minutes each and blocked in 2% BSA, and 0.3% Triton-X in 1X PBS for 1 hour. Incubation with the primary antibody was done overnight at 4 ºC. Post-primary staining, the samples were washed 4 times for 10 min in 1X PBS containing 0.3% Triton-X and incubated with the appropriate fluorescent secondary antibody for 1 hour at room temperature in the dark. The ovaries were then washed and mounted using 70% glycerol with n-propyl gallate. One animal was mounted per coverslip to count a number of ovarioles and variation in the phenotype per animal. DAPI (Invitrogen Molecular Probes) was used to stain the nuclei at 1:500 dilution. Anti-orb was (1:20) was from DSHB, Iowa, USA; all secondary antibodies (1:1000) and Phalloidin 488 (1:100) were from Molecular Probes. Images were taken on Zeiss 710 LSM confocal microscope and Leica SP8 confocal microscope using a 40X oil objective and subsequently processed using Image J software. GraphPad Prism was used for statistical analyses. Student's T-Test was applied for each set of analyses.

3) Western Blotting:

Western blotting was carried out using standard methods. Briefly, 10-15 adult fly ovaries were collected and homogenized immediately in RIPA buffer containing phosphatase inhibitor cocktail (Sigma-Aldrich). The lysates were centrifuged at 21000 x g to remove tissue debris; the supernatant was loaded onto to a 10% Acrylamide SDS-PAGE gel with a 5% Stacking Gel at 80-125 Volts. Bio-Rad Precision Plus Protein™ Dual Color Standard (10-250kDa) was used as a molecular weight marker. Transfer of the proteins onto a PVDF membrane was done overnight at 4°C, at 120mA. The blot was activated with methanol for 5 minutes prior to transfer. Ponceau staining was done to check for the efficiency of the transfer.

Blocking was carried out in 5% skimmed milk in 1X TBST containing 0.1% Tween-20 for 1 hour at room temperature. Primary antibody was added to the blot and incubated at room temperature or 4°C for 3 hours or overnight respectively with slow agitation. Anti- Orb (1:200 dilution, DSHB, Iowa.), Mouse anti-tubulin DM1A (1:20,000, Sigma) were used. Blots were washed 3x 15 minutes with 1X TBST. HRP (Horse Radish Peroxidase) conjugated secondary antibodies were used at 1:10,000 dilution (Jackson Immunoresearch). The Blot was developed using Chemiluminescent Substrate Kits (Millipore® Immobilon Western Chemiluminescent HRP Substrate/ Luminata Crescendo Western HRP substrate/ Luminata Classico Western HRP substrate), and images were acquired using LAS4000 imaging system.

4) RT-PCR:

Adults ovaries were dissected in chilled 1x PBS. RNA isolation was carried out using Trizol reagent(Invitrogen) as per the manufacturer's instructions. The lysates were vortexed for 10 seconds; Chloroform (1/5 volume of Trizol), was added and the samples were kept static for 5 minutes and centrifuged at 12000 x g at 4°C. The top layer was taken into a fresh Eppendorf tube. An equal volume of 70% ethanol was added and mixed gently and added to the RNA isolation column. These were centrifuged at 12000 x g for 30seconds; columns were washed with 700µl of Wash Buffer I from Invitrogen Kit by centrifugation at 12000 x g for 15seconds. This was followed by two washes with 500µl with Wash Buffer II. RNAase free water (30-40ul) was added to the column and kept for 30 minutes. RNA was eluted through

centrifugation for (approximately 2 minutes). RNA samples were subjected to DNAase treatment to get rid of any genomic DNA.

DNAse treated RNA samples were used for the RT reaction. Equal amounts of RNA (1ug) were used for the RT reaction.

The following 20µl reaction mixture was used.

10x buffer	2µl
25x dNTPs	0.8µl
10x random primers	2µl
RNA sin	1µl
RT (reverse transcriptase)	1µl
Nuclease-free water	3.2µl
RNA templates	10µl (max1µg RNA)

PCR program employed for the cDNA synthesis is given below:

Steps	**Temperature**	**Duration**
Primers extension	25°C	10 minutes
cDNA synthesis	37°C	120minutes
Reaction termination	85°C	5minutes
Cooling of the samples	4°C	Hold

Real-time PCR was performed for *rp49* and *orb* with SYBR green mix (Kappa Biosystem) on an Eppendorf RealPlex2. The fold change was calculated using $2^{-\Delta(\Delta CT)}$

The following primer pairs were used for real-time PCR,

>RP49_Forward	GACGCTTCAAGGGACAGTATC
>RP49_Reverse	AAACGCGGTTCTGCATGAG
>Orb _Forward	GAGTGGGAAAGGGAAGGTAC
>Orb _Reverse	CAGGTAGGAGCTTATCGAGTG
>Dilp1 _Forward	GGTGTGTCCCCATGGCTTTA
> Dilp1_Reverse	TGCTGCTATCATCCTGCACC
> Dilp2 _Forward	CGAGGTGCTGAGTATGGTGTG
> Dilp2 _Reverse	CCCCAAGATAGCTCCCAGGA

> Dilp3 _Forward	ATGGGCATCGAGATGAGGTG
> Dilp3_Reverse	CGTTGAAGCCATACACACAGAG
> Dilp4_Forward	ATGAGCCTGATTAGACTGGGAC
> Dilp4_Reverse	TCTAGCATCCTTAGACGCACT
> Dilp5 _Forward	TGCCTGTCCCAATGGATTCAA
> Dilp5_Reverse	GCCAAGTGGTCCTCATAATCG
> Dilp6 _Forward	GTCCAAAGTCCTGCTAGTCCT
> Dilp6_Reverse	TCTGTTCGTATTCCGTGGGTG
> Dilp7_Forward	AGGAGGGTCTCGAGATGCTT
> Dilp7_Reverse	CCCAATATAGCTGGCGGACC
> Dilp8 _Forward	GGACGGACGGGTTAACCATT
> Dilp8_Reverse	CATCAGGCAACAGACTCCGA

5) Isolation of hemolymph:

To isolate haemolymph, flies of the appropriate genotype were pierced in the thoracic region using a dissecting needle. The injured flies were put in a 0.6 ml tube containing a hole at the bottom and placed in a 1.5 ml Eppendorf tube. The haemolymph was collected centrifuging the animals at 4°C for 20 minutes at 6000 x g to 8000 x g. The haemolymph samples were further processed for western blotting as described above.

6) Protein expression for antibody generation

pGEX-Mon1 was transformed into BL21(DE3) and grown overnight on an ampicillin-dosed LB agar plate (0.1 mg/ml ampicillin) at 37°C. A single, isolated colony was used to grow a 1 ml primary culture. 50 ml secondary cultures were inoculated using 500 µl of primary culture and allowed to grow at 37°C with agitation until OD600 0.5-0.8. Induction with IPTG at a final concentration of 1 mM was for 6 hours at 25°C. 800 µl of culture was used to test for expression using SDS-PAGE. The remaining sample was centrifuged, and the pellet was frozen for subsequent purification.

For purification of the protein, the pellet was suspended in lysis buffer having 100 mM NaCl, 50 mM Tris, 1mM EDTA, 2 mM DTT, 0.25mg/ml lysozyme, 1mM phenylmethylsulfonyl fluoride (PMSF), and 1x protease inhibitor cocktail from Sigma-Aldrich. For 50ml bacterial pellet, 2ml lysis buffer was added. The cells were incubated on the nutator for 30-45 minutes at 4°C and sonicated at 60% amplitude for 45seconds

in pulses of 1second ON and 3seconds OFF. The sonicated lysate was centrifuged for 30-45 minutes at 4°C at 12000 x g. The supernatant was added to glutathione agarose beads (ThermoFisher Scientific) equilibrated with extraction buffer containing 100mM NaCl, 50mM pH 8.0 Tris, 1mM EDTA and kept on a nutator overnight at 4°C. After incubation, a small volume of the beads was washed 3-4 times with extraction buffer and boiled in 80µl extraction buffer + 20µl 5X SDS sample buffer for 10 minutes at 95°C. 20µl of sample was run on a 10% SDS-PAGE gel and stained with Coomassie Brilliant Blue to check for binding. The protein-bound glutathione beads were incubated in 10mg/ml thrombin (HiMedia) overnight at 4°C on a nutator. The eluate was collected, and the beads were washed twice with 0.1% TBST, with eluates being collected each time. Each eluate was analyzed by SDS-PAGE to determine elution of the protein.

Sub-cloning of Mon1 into pET28a vector and protein induction:

Sub-cloning of Mon1 from pGEX vector into pET28a was done using standard molecular biology techniques. The primers used for PCR and cloning are given below.

> Mon1 _Forward	ATGCGAATTCATGGAAGTAGAGCAGACGTC
> Mon1 _Reverse	ATGCGCGGCCTTAGAATGTGGCATGGTTTCGT

Protein induction was carried out as described above. Affinity purification was tested using Ni-NTA beads. Elution from the beads was done using 1x PBS containing 250mM Imidazole.

7) Insulin feeding:

Homozygous *Dmon1*$^{\Delta 181}$ exhibit a half-life of approximately 3 days; the animals fail to survive beyond a week. To determine the dose of insulin, mutant animals were kept on regular cornmeal medium containing varying amounts of insulin ranging from 0.5µg/ml - 20µg/ml (0.5, 1, 3, 5, 10 15, 20). At 3µg/ml, 10µg/ml and beyond, the flies failed to survive longer than 4 days. Survival of the mutants was best at 5µg/ml. At this dose, the animals survived for at least 10 days with a half-life of approximately 5-6 days. Based on this, the dose of 5µg/ml of insulin was used for all subsequent experiments. The ovaries of animals kept on insulin medium were examined in 5 and 10 day old flies. Non-insulin treated mutant animals were used as controls.

3. RESULTS

3.1. Mon1 mutants are sterile and have reduced ovaries.

It was previously observed that homozygous *Dmon1* $^{\Delta 181}$ mutant escapers are short lived and sterile (Deivasigamani et al., 2015 and personal communication). Detailed observation showed that these animals are also smaller in size (Figure3.1.1A&B). We measured the length of mutant female flies and compared them to age-matched wildtype females. The mutants were found to be significantly smaller in size as compared to the control: 2397.82±108.94 µm in control versus 1886±68.39 µm in the mutant (Figure 3.1.1C).

The sterility in *Dmon1* $^{\Delta 181}$ mutants was observed in both, males and females. To find out whether this defect is allele specific, different allelic combinations of the mutant were examined for sterility. Female homozygous *Dmon1* $^{\Delta 181}$ adults, as observed previously, were sterile. Heterozygous *Dmon1* $^{\Delta 181}$/+ are fertile and non-lethal which indicates that one copy of *Dmon1* is sufficient for viability. *pog*^{1} is an EMS allele of *Dmon1.* These animals die during early second instar larval stage (Basargekar and Ratnaparkhi., personal communication). We checked the fertility of *Dmon1* $^{\Delta 181}$/*pog*^{1} and *Dmon1* $^{\Delta 181}$/*Df(2L)9062* escapers. Both these allelic mutants showed poor viability and were found to be sterile. A summary of these observations is shown in Table1. This suggests that loss of *Dmon1* leads to sterility.

Figure 3.1.1

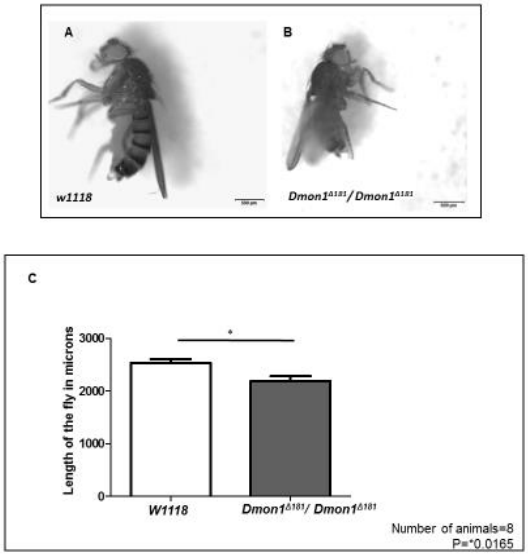

Figure 3.1.1: *Dmon1* $^{\Delta 181}$ mutants are small.
(A) Wild type female fly.
(B) *Dmon1* $^{\Delta 181}$/*Dmon1* $^{\Delta 181}$ mutant female.
(C) Graph showing the difference in length between wildtype and mutant flies. Mutants show a small but significant decrease in body length.

Table 3.1.1: Lethality and fertility observed in different allelic mutants of *Dmon1*.

Genotype	Lethality	Fertility
Dmon1 $^{\Delta 181}$/ +	Non-lethal	Fertile
Dmon1 $^{\Delta 181}$/*Dmon1* $^{\Delta 181}$	Lethal with few escapers	Escapers are sterile
pog^{1}/*pog*^{1}	Lethal	-----
Dmon1$^{\Delta 181}$/*pog1*	Lethal with few escapers	Escapers are sterile
Dmon1 $^{\Delta 181}$/*Df(2L)9062*	Lethal with few escapers	Escapers are sterile

Next, the ovaries in homozygous *Dmon1* $^{\Delta 181}$ mutants were observed. Interestingly, the ovaries in these animals were found to be extremely small. This phenotype was also observed in *Dmon1* $^{\Delta 181}$ /*Df(2L)9062* and *Dmon1* $^{\Delta 181}$ /*pog*^{1} mutants (Figure 3.1.2A-D). The difference in size was quantitated by measuring the length of the ovary from the proximal to distal end. The average length of the ovary in wildtype animals was found to be 1399.70µm. In case of each of the mutants the length was found to be more than 65% smaller: *Dmon1* $^{\Delta 181}$ / *Dmon1* $^{\Delta 181}$ (431.015 ±87.16 µm); *Dmon1* $^{\Delta 181}$ */Df(2L)9062* (571.53±82.21 µm); *Dmon1* $^{\Delta 181}$ /pog^{1} (711.347±153.21 µm) (Figure 3.1.2E).

Drosophila adult females have a pair of ovaries, each of which contains 16-20 ovarioles. The ovarioles are the structural and functional units of the ovary. Each ovariole has a string of six to eight sequentially developing egg chambers with 14 defined stages of maturation. To check if *Dmon1* mutants also show a change in ovariole number, we counted the number of ovarioles in each mutant ovary. The average number of the ovarioles in wildtype animals was found to be 34.5±1.5. In *Dmon1*$^{\Delta 181}$/ *Dmon1*$^{\Delta 181}$, *Dmon1*$^{\Delta 181}$/ *Df(2L)9062* mutants, ovarioles were significantly reduced in number (*Dmon1* $^{\Delta 181}$ / *Dmon1* $^{\Delta 181}$ (21.3 ±3.5); *Dmon1* $^{\Delta 181}$ /*Df(2L)9062* (32.4±2.31)). However, *Dmon1* $^{\Delta 181}$ /*pog*^{1} (35.3±1.4) did not show any change in ovariole number (Figure 3.1.2F).

Figure 3.1.2

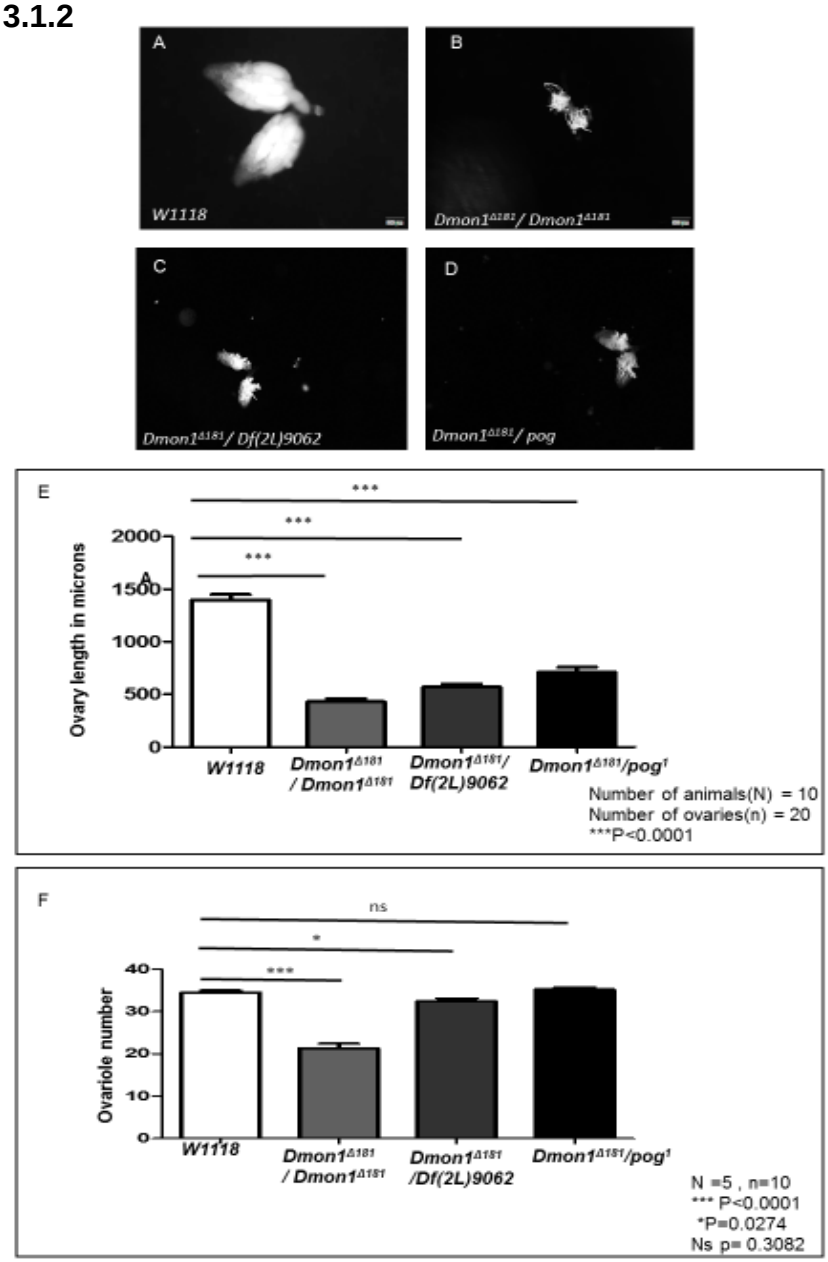

Figure3.1.2. **Characterization of the ovarian morphology in *Dmon1* mutants.**

(A) Wild type ovary.

(B-D) Ovaries of *Dmon1$^{\Delta 181}$/ Dmon1$^{\Delta 181}$*, *Dmon1$^{\Delta 181}$/ Df(2L)9062, Dmon1$^{\Delta 181}$/pog^{1}* alleles.

(E) Graph showing the length of the ovaries measured in wildtype and mutant animals. All allelic combinations of Mon1 mutants show significantly smaller ovaries.

(F) Quantitation of ovariole number. *Dmon1$^{\Delta 181}$/ Dmon1$^{\Delta 181}$*, *Dmon1$^{\Delta 181}$/ Df(2L)9062* mutants show a significant decrease in ovariole number while the number in *Dmon1$^{\Delta 181}$/pog^{1}* mutants is comparable to control animals.

3.2. *Dmon1 mutant* egg chambers exhibit stalling and degeneration.

Each ovariole in an ovary consists of a germarium at the distal end with egg chambers containing the oocyte and 15 nurse cells at different stages of maturation with the youngest stage being near the germarium. The specification of the oocyte or egg is associated with the accumulation of transcripts of *Orb, BicD, Egl and Cup* in one of the 16 cells in a cyst (Johnston *et al.,2000)*. To get a better understanding of the ovarian phenotype in *Dmon1* mutants, we stained mutant ovaries from 2-3 day old animals with phalloidin that labels actin, anti-Orb, and DAPI to stain nuclei. Ovaries from age-matched wildtype animals were used as a control.

As with overall ovary size, homozygous *Dmon1*$^{\Delta 181}$mutant ovaries showed extremely small ovarioles compared to control (Figure 3.2.1). In addition, most of the ovarioles showed arrested the development of the egg chamber at stage 7-8 with very few egg chambers at stage 9-10. This phenotype was quantified by scoring each ovariole for all the different stages. In wildtype, all developmental stages are present from germarium to egg stage (Figure 3.2.2A). In homozygous *Dmon1* $^{\Delta 181}$mutants, very few ovarioles show egg chambers at stage 7-8. Most of the time, stalling was observed at stage 7-8, and no eggs are seen (Figure 3.2.2B). A similar trend was seen in ovarioles from *Dmon1* $^{\Delta 181}$*/Df(2L)9062* and *Dmon1* $^{\Delta 181}$*/pog*^{1} although these animals showed a few ovarioles with egg chambers at stage 9-10 egg (Figure 3.2.2C-D). As with *Dmon1* $^{\Delta 181}$ mutants, the percentage of egg formation in these mutants was also very low.

Figure 3.2.1

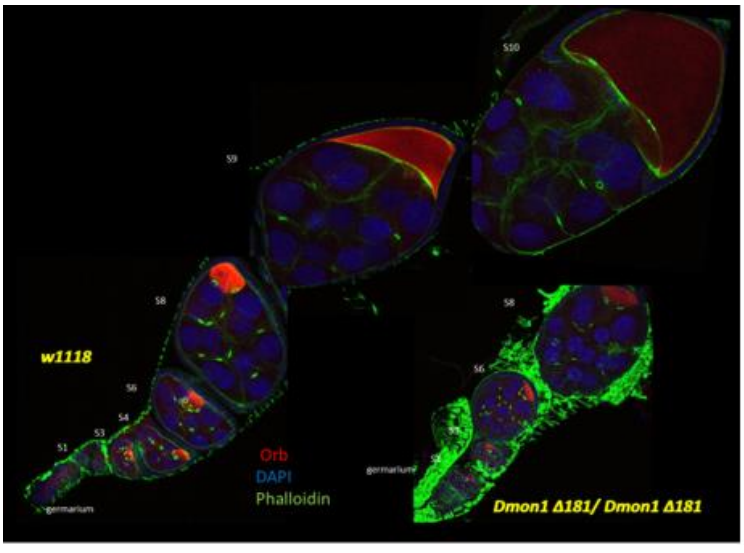

Figure 3.2.2

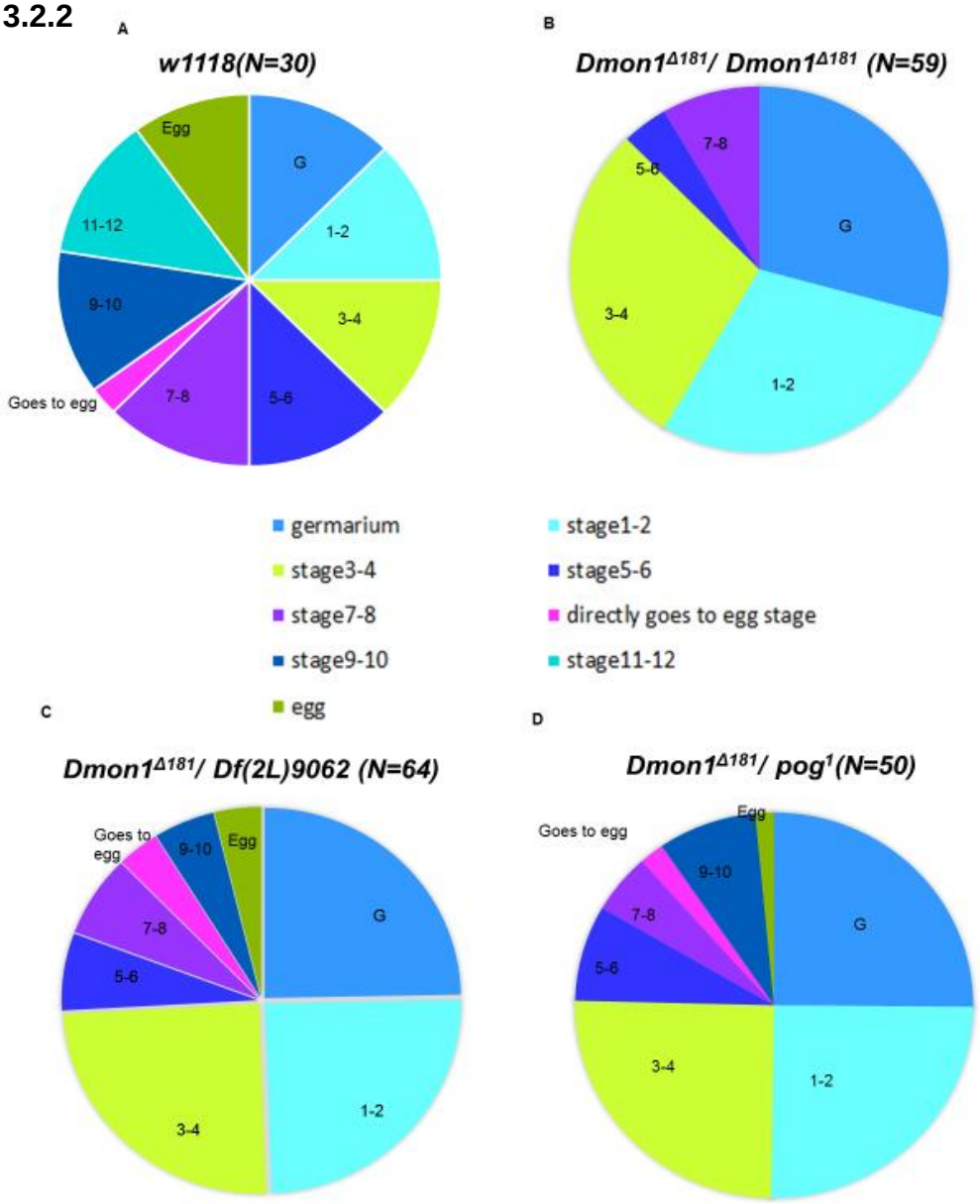

Figure3.2.1: *Dmon1* $^{\Delta 181}$ mutants have small ovarioles.

Representative image of a wildtype ovariole showing egg chambers from germarium to stage 10. DAPI(blue) stained nuclei, phalloidin (green) stained actin and Orb expression is in the red. Mutant ovariole of showing egg chambers from germarium to stages 6 and 8. No late stages and egg formation are seen in these mutants.

Figure3.2.2: Pie charts showing the occurrence of the different stages of egg chambers in wildtype and *Dmon1* mutant ovarioles.

(A) Note that near equal distribution of all stages in wild type ovarioles.

(B-D) All mutant allelic combinations show stalling of egg chambers at stages 7-8. Very few ovarioles show the presence of egg chambers older than stage 8. In *Dmon1*$^{\Delta 181}$/ *Dmon1*$^{\Delta 181,}$ late stages and egg

formation are not seen whereas in other *Dmon1*$^{\Delta 181}$*/ Df(2L)9062, Dmon1*$^{\Delta 181}$*/pog*^{1} alleles, very few ovarioles show late stages and egg formation.

Another interesting phenotype observed in *Dmon1* mutants was degeneration of egg chambers (Figure 4). Degeneration is defined by three parameters: (a) Mislocalization of Orb, (b) disorganized actin filaments and (c) fragmented nucleus. Approximately 10-14 % of the mutant ovarioles showed degenerating egg chambers (Figure 3.2.3C). In most cases, the degeneration was observed in the terminal egg chamber (Figure 3.2.3B).

Figure 3.2.3

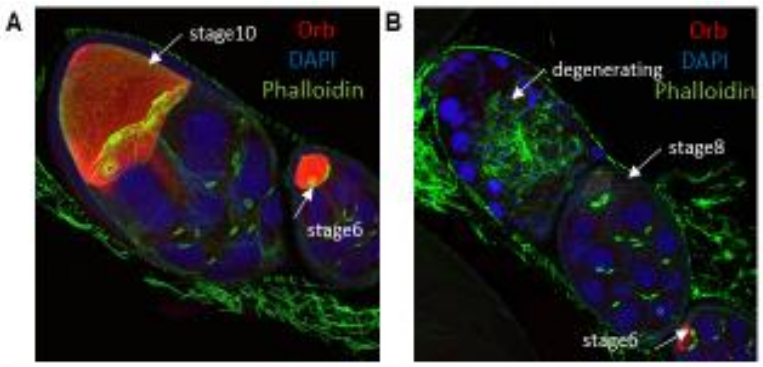

C

Genotype	Percentage of Degeneration
Dmon1 $^{\Delta 181}$***/Dmon1*** $^{\Delta 181}$	13.5%
Dmon1$^{\Delta 181}$***/pog1***	12%
Dmon1 $^{\Delta 181}$***/Df(2L)9062***	11%

Figure 3.2.3: *Dmon1* mutant ovarioles exhibit degeneration.

(A) Representative image of a wildtype ovariole showing egg chambers at stages 6 and 10. Orb expression is in the red.

(B) Mutant ovariole of showing egg chambers at stages 6 and 8. The terminal egg chamber show degeneration.

(C) Quantitation of the degeneration phenotype. All allelic mutants exhibit degeneration in approximately 10-14% of the ovarioles.

3.3. *Orb* levels are down regulated in *Dmon1$^{\Delta 181}$ mutants.*

Next, we examined the level of Orb in the developing egg chambers. Orb is an RNA-binding protein involved in the specification of the oocyte. It is responsible for localization of *gurken(gur) and Oskar(osk)* which in turn, are required for dorsoventral(D-V) and anterioposterior(A-P) patterning of the oocyte (Lantz *et al.,*1994*).* In the developing egg chamber, Orb is present in a crescent-like manner at the posterior end of the oocyte. Examination of Orb expression showed that levels of this protein are reduced in *Dmon1$^{\Delta 181}$* mutants (Figure 3.3.1).

Figure 3.3.1

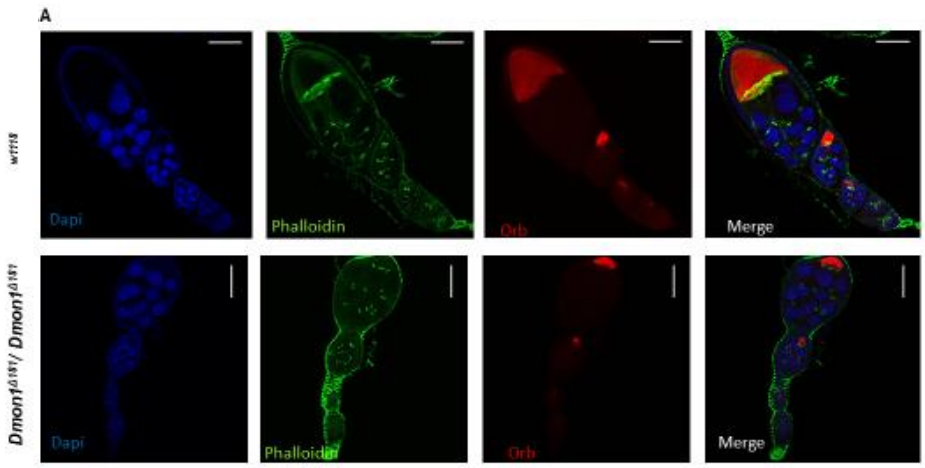

Figure3.3.1: Expression of Orb is reduced in *Dmon1$^{\Delta 181}$* mutants.

Representative image of a wildtype ovariole showing egg chambers from germarium to stage 10. DAPI(blue) stained nuclei, phalloidin (green) stained actin and Orb expression is in the red. Mutant ovariole of showing egg chambers from germarium to stages 6 and 8. No late stages and egg formation are seen in these mutants.

To confirm this, quantitative RT-PCR for *orb* was done using RNA isolated from 2-3 day old ovaries of *Dmon1$^{\Delta 181}$* mutants and age-matched wildtype animals. We found that the levels of *orb* mRNA are reduced in *Dmon1$^{\Delta 181}$* mutants. The decrease was found to be more than two-fold compared to wildtype (Figure 3.3.2A). We also checked for the decrease in Orb protein by Western blotting. To do this, we took an equal weight of wildtype and mutant ovaries and generated a lysate using an equal volume of lysis buffer and loaded an equal volume of the lysate for a Western blot. In this experiment case, a decrease in Orb levels was seen in the lysate from mutant ovaries. However, the tubulin levels were also low (Figure 3.3.2B). This was

consistently observed. To be able to make meaningful comparisons, we loaded varying volumes of the protein lysate from wildtype ovaries along with the mutant lysate whose volume was twice the maximum volume loaded for the wildtype sample. The amount of tubulin in the mutant sample was found to be greater than that observed in the lane with a maximum volume of the wildtype lysate (Figure 3.3.2C). Despite the high levels of tubulin, the amount of Orb in the mutant sample was much lower than the controls suggesting that Orb protein is indeed low in *Dmon1*$^{\Delta 181}$ mutants.

Figure 3.3.2A

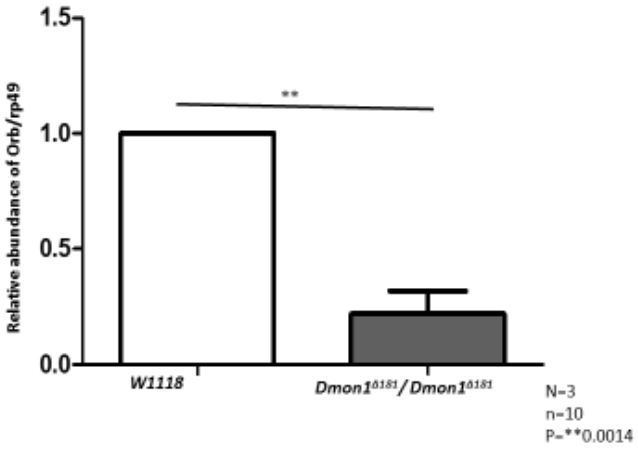

Figure 3.3.2

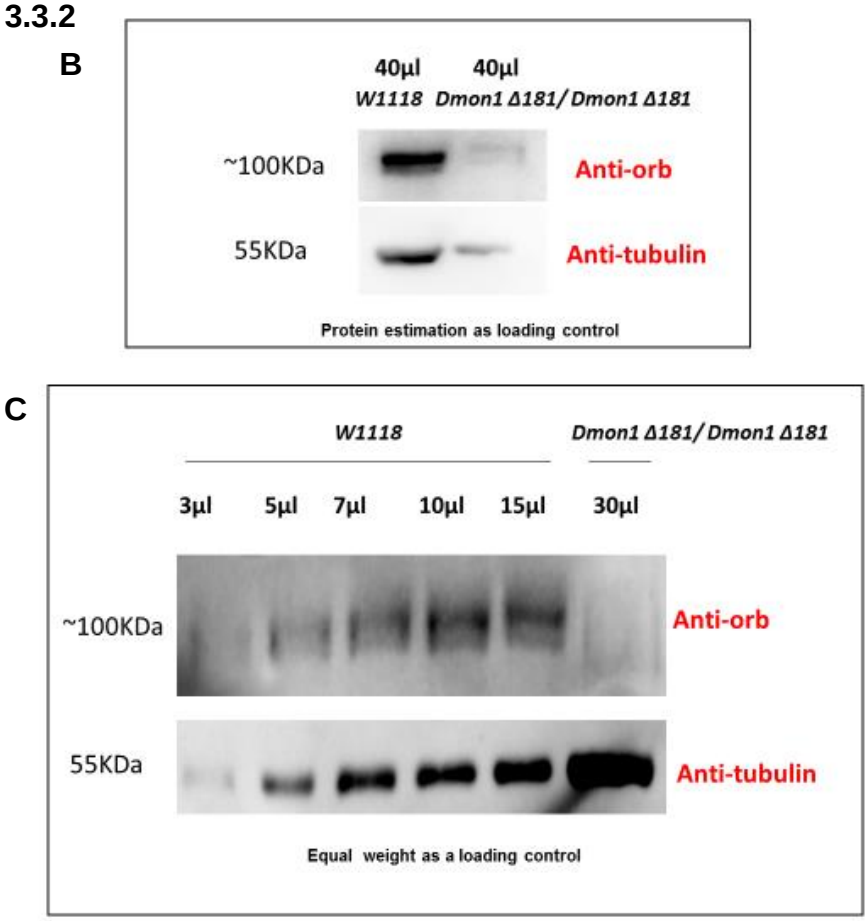

Figure3.3.2: Quantitative RT-PCR and Western blot to measure Orb levels in mutant ovaries.
(A) Graph showing the abundance of Orb mRNA normalized to ribosomal protein transcript rp49. More than a twofold decrease in Orb levels is seen in mutant *Dmon1*$^{\Delta 181}$/ *Dmon1*$^{\Delta 181}$ ovaries.
(B-C) Western blot was done using anti-Orb on lysates from wildtype and mutant *Dmon1*$^{\Delta 181}$/ *Dmon1*$^{\Delta 181}$ ovaries. Anti-tubulin was used as a loading control. Despite the high levels protein in mutant lysates, Orb levels were found to very low compared to wildtype lysates.

3.4. *Dmon1*$^{\Delta 181}$/ *Dmon1*$^{\Delta 181}$ mutant phenotype is rescued by expression of Mon1 in neurons.

The studiy from our lab showed that pan-neuronal expression of *Dmon1* rescues the lethality of *Dmon1*$^{\Delta 181}$ mutants (Devasigamani *et al 2015)*, also rescues the gross ovary size. To determine the nature and extent of rescue, we stained these ovaries with phalloidin, anti-Orb, and DAPI. As seen previously, neuronal expression of *Dmon1* led to the rescue of ovary size (Figure 3.4.1B). Interestingly, this also rescued

the ‘stalling’ phenotype observed in the ovarioles. Ovaries from (C155; *Dmon1$^{\Delta 181}$/ Dmon1$^{\Delta 181}$*; *UAS-Dmon1::HA*) showed the presence of egg chambers at all stages of development including mature eggs (Figure 3.4.1C).

Figure3.4.1

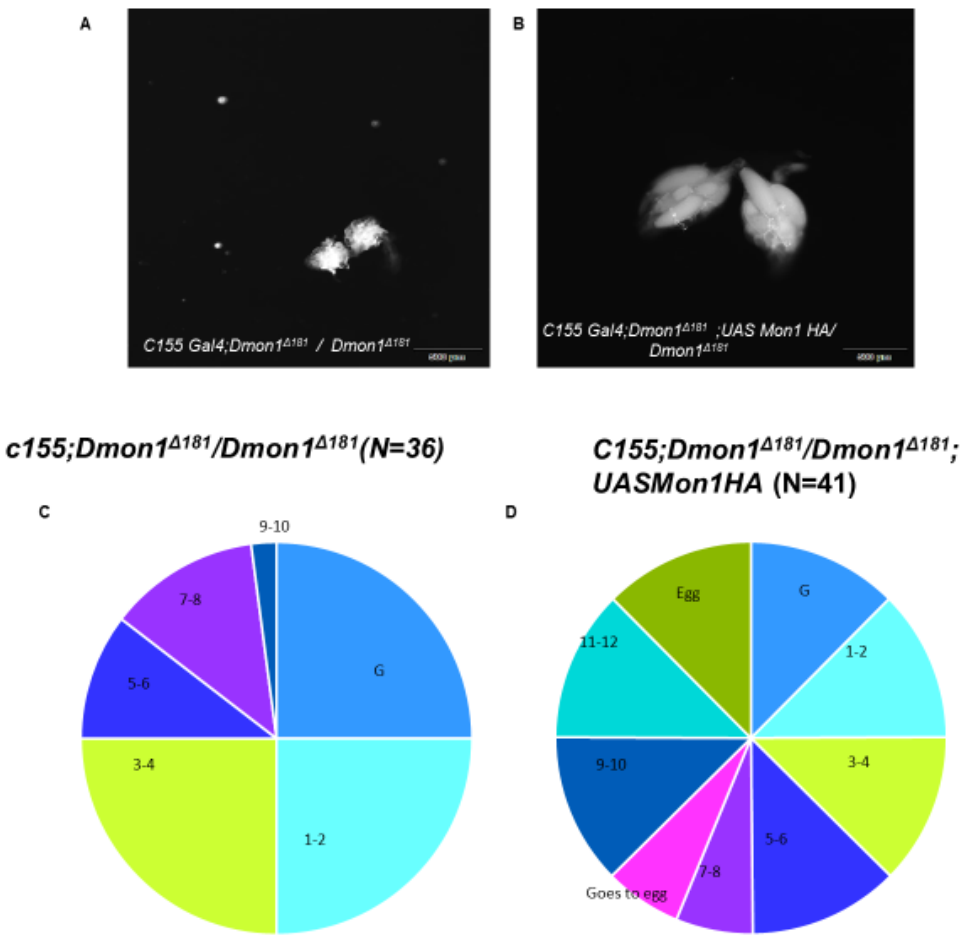

Figure 3.4.1: The ovary phenotype in *Dmon1$^{\Delta 181}$* mutants is rescued by expression of *Dmon1* in neurons.

(A) Control ovaries of the genotype *c155; Dmon1$^{\Delta 181}$/Dmon1$^{\Delta 181}$*.

(B) Ovaries of *C155; Dmon1$^{\Delta 181}$/Dmon1$^{\Delta 181}$; UAS-Dmon1::HA.* Note the increase in the size of the ovaries.

(C-D) Pie charts showing the distribution or occurrence of the different stages of egg chambers in *C155; Dmon1$^{\Delta 181}$/Dmon1$^{\Delta 181}$* (control) and *C155; Dmon1$^{\Delta 181}$/Dmon1$^{\Delta 181}$; UAS-Dmon1::HA* (rescue) ovarioles.

The ovary receives innervation only from octopaminergic neurons. The innervation is made to the peritoneal muscle sheath that covers the entire ovary. No direct innervation is present to the ovary itself (Middleton *et al.,*2006). We checked if the expression of *Dmon1* in octopaminergic neurons rescues the ovary phenotype. Indeed, expression of *Dmon1* in octopaminergic neurons using *tdc2*-GAL4 rescued lethality as well as all the ovary defects present in *Dmon1*$^{\Delta 181}$. As shown in figure 3.4.2, all aspects of the ovary phenotype such as size, ovariole number, degeneration, and stalling of egg chambers were rescued.

Figure3.4.2

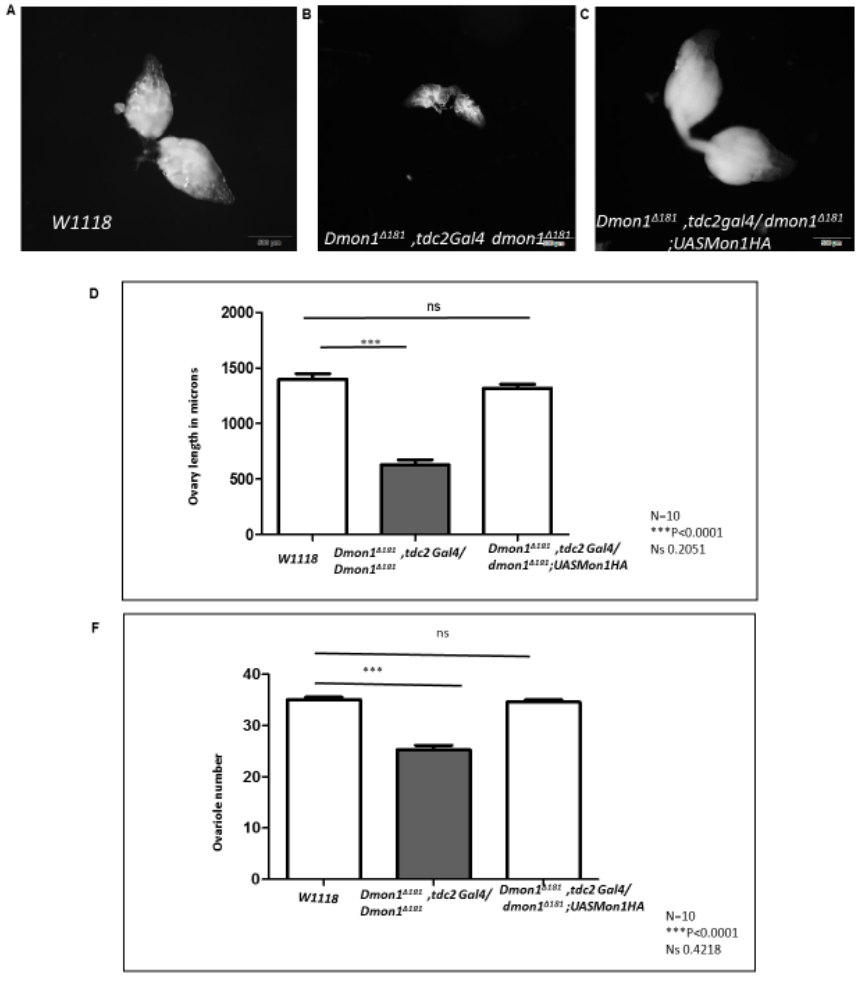

Figure 3.4.2: Expression in octopaminergic neurons is sufficient to rescue ovary size and ovariole number in *Dmon1*$^{\Delta 181}$ mutants.

(A) Wildtype ovaries

(B) *tdc2-GAL4, Dmon1*$^{\Delta 181}$*/Dmon1*$^{\Delta 181}$ ovaries or control ovaries.

(C) Ovaries of *tdc2-GAL4, Dmon1*$^{\Delta 181}$*/Dmon1*$^{\Delta 181}$*; UAS-Dmon1::HA.* Note the rescue of size.

(D) Graph showing the length of the ovaries measured in wildtype, *tdc2-Gal4, Dmon1$^{\Delta 181}$/Dmon1$^{\Delta 181}$* and rescue. *Tdc2-Gal4, Dmon1$^{\Delta 181}$/Dmon1$^{\Delta 181}$; UAS-Dmon1::HA* animals show rescue of ovary length same as wildtype.

(F) Quantitation of ovariole number. *Tdc2-Gal4, Dmon1$^{\Delta 181}$/Dmon1$^{\Delta 181}$* ovaries mutants show a significant decrease in ovariole number; whereas *tdc2-Gal4, Dmon1$^{\Delta 181}$/Dmon1$^{\Delta 181}$; UAS-Dmon1::HA* restores the ovariole number. In the rescue experiment, the ovariole number of *tdc2-gal4, Dmon1$^{\Delta 181}$/Dmon1$^{\Delta 181}$;UAS-Dmon1::HA* is same as wildtype.

We examined Orb levels in mutant ovarioles rescued by *tdc2*-GAL4. As shown in Figure 3.4.3A, ovarioles from mutant control animals show low Orb levels. The expression was restored in the rescue animals. The 'stalling' phenotype observed in mutant ovarioles is also rescued (Figure3.4.3B-C).

Figure3.4.3 A

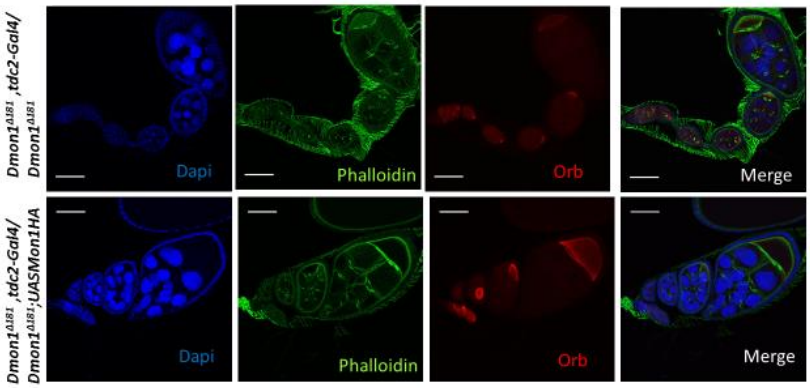

B

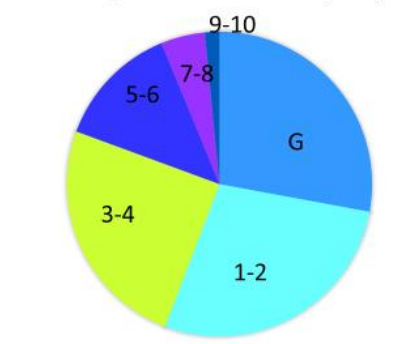

C

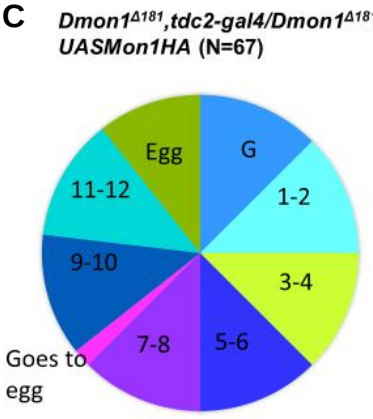

Figure3.4.3: Expression of *Dmon1* in octopaminergic neurons rescues Orb levels and the stalling defects.

(A)Representative image of a *tdc2-Gal4, Dmon1$^{\Delta 181}$/Dmon1$^{\Delta 181}$* ovariole showing egg chambers from germarium to stage 8. DAPI(blue) stained nuclei, phalloidin (green) stained actin and Orb expression is in the red. *Tdc2-Gal4, Dmon1$^{\Delta 181}$/Dmon1$^{\Delta 181}$; UAS-Dmon1::HA* ovariole of showing egg chambers from germarium to stages 10, late egg chamber is seen in the rescue.

(B-C) Pie charts are showing the distribution of the occurrence of the different stages of egg chambers in *tdc2-Gal4, Dmon1$^{\Delta 181}$/Dmon1$^{\Delta 181}$* and *tdc2-Gal4, Dmon1$^{\Delta 181}$/Dmon1$^{\Delta 181}$; UAS-Dmon1::HA* ovarioles. *Tdc2-Gal4, Dmon1$^{\Delta 181}$/Dmon1$^{\Delta 181}$* show stalling of egg chambers at stages 7-8. Very few ovarioles show the presence of egg chambers older than stage 8. In *tdc2-Gal4, Dmon1$^{\Delta 181}$/Dmon1$^{\Delta 181}$; UAS-Dmon1::HA* late stages and egg formation is seen.

3.5. Neuronal knock-down of Mon1 is sufficient to give ovary phenotype.

Since neuronal expression of *Dmon1* was able to rescue the ovary phenotype, we decided to check if knock-down of the gene in neurons was sufficient to produce small ovaries. We used the UAS-GAL4 system to knock-down *Dmon1* in neurons using RNAi. Expression of ds*Dmon1* RNA in all neurons using a pan-neuronal driver (*C155*-Gal4) produced the small ovary phenotype at both 25 and 29 degrees. Similar results were obtained with *tdc2*-Gal4. We measured the length of the ovaries in each case and found them to be significantly smaller in size as compared to their respective controls. This suggests that at least size of the ovary is neuronally regulated by *Dmon1.*

Figure3.5.1

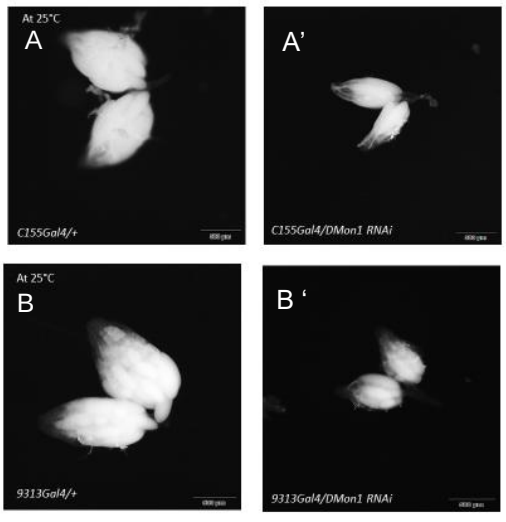

Figure3.5.1: **Neuronal knock-down of Mon1 is sufficient to reduce ovary size.**
(A & A') Wild type ovary(C155>+) and pan-neuronal knock-down of Mon1 ovary at 25**°C**.
(B & B') Wild type ovary and subset of neuronal knock-down of Mon1(*tdc2Gal4>Mon1RNAi*) ovary at 25**°C**.

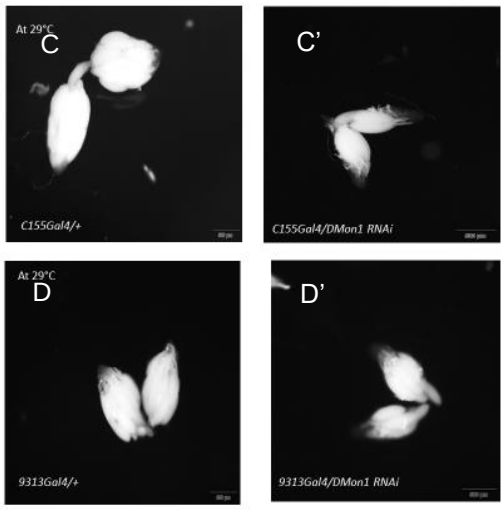

(C & C') Wild type ovary and neuronal knock-down of Mon1(*c155>Mon1RNAi*) ovary at 29**°C**.

(D & D') Wild type ovary and knock-down of Mon1(*tdc2-Gal4>Mon1RNAi*) ovary at 29**°C**.

In all combinations of Mon1 knock-down at both 25**°C** and 29**°C** show significantly smaller ovaries.

Figure3.5.2

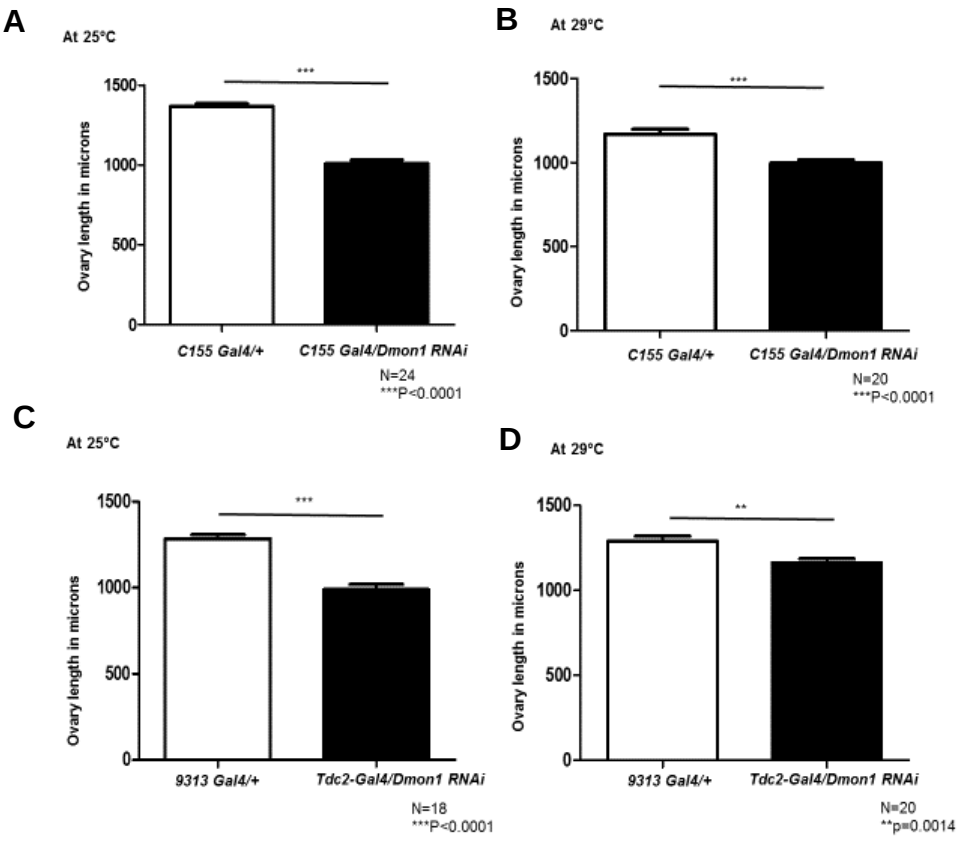

Figure3.5.2: Quantitation of ovary length in *Dmon1* RNAi animals. Graphs showing the length of the ovaries measured in wildtype and know down animals. All combinations at both 25°C and 29°C of *Dmon1* knock-down at different temperature mutants significantly smaller ovaries.

(A) Wildtype ovary length (C155/+) is1366.83 µm and pan-neuronal knock-down of Mon1 ovary is1006.9 µm at 25°C.

(B) Wildtype ovary length is 1284.85 µm, and pan-neuronal knock-down of Mon1(*9313/Mon1RNAi*) ovary length is 988.33 µm at 25°C.
(C) Wildtype ovary length is 1170.185 µm and ovary specific neuronal knock-down of Mon1(*c155/Mon1RNAi*) ovary length 998.31 85 µm at 29°C.
(D) Wildtype ovary length is 1290.41µm, and ovary specific neuronal knock-down of Mon1(*9313/Mon1RNAi*) ovary length is 1161.5 µm at 29°C.

In contrast, knock-down of *Dmon1* in the germline using germline-specific drivers (Mat-Gal4 and nanos-Gal4) did not produce any ovary phenotype at 25 degrees. We measured the length of the ovaries and found no change in ovary size compared to control ovaries. This suggests that control of ovary size is non-cell autonomous.

Figure3.5.3

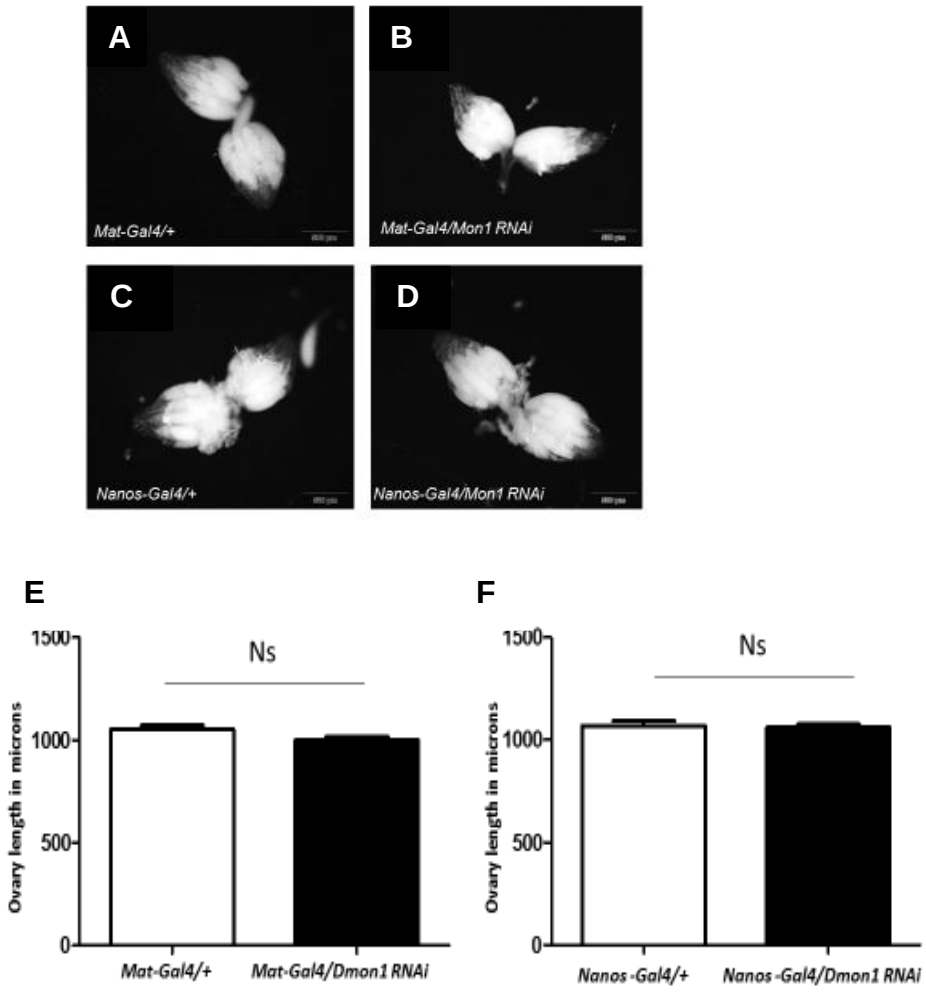

Figure3.5.3: **Knock-down of *Dmon1* in ovarian germline does not alter ovary size.**

(A & B) Wildtype ovary(Mat-Gal4/+) and germline-specific knock-down of Mon1 *(Mat-Gal4/Mon1RNAi*) ovary at 25**°C**.

(C & D) Wildtype ovary(Nanos-Gal4/+) and germline-specific knock-down of Mon1(*Nanos-Gal4/Mon1RNAi*) ovary at 25**°C**.

Graphs showing the length of the ovaries measured in wildtype and knock-down animals.

(E) Wildtype ovary(Mat-Gal4/+) is 1051.3 µm, and germline-specific knock-down of Mon1 *(Mat-Gal4/Mon1RNAi*) ovary is 1001.036 µm at 25**°C**. (No. of ovaries=10)

(F) Wildtype ovary(Nanos-Gal4/+) is 1067.73 µm, and germline-specific knock-down of Mon1(*Nanos-Gal4/Mon1RNAi*) ovary is 1060.61 µm at 25**°C**. (No. of ovaries=10)

3.6. Dilps are affected in the *Dmon1$^{\Delta 181}$* mutant.

Insulin/ insulin-like signaling in *Drosophila* is highly conserved. IIS pathways regulate growth, development, metabolism, reproduction and stress response. There are eight *dilps* encoding *Drosophila*- insulin-like peptides, but only one receptor is present for all the dilps which are the DInR receptor. Different *dilps* localize to different cell types and tissues to perform cell and stage-specific functions (Nassel,2013).

	LOCATION		
DILPs	**LARVAE**	**ADULT**	**AXON TERMINATION**
DILP1	IPCs	-------	---------
DILP2	IPCs Salivary Glands Imaginal Disc Glial cells of CNS	IPCs	Brain neuropil Corpora cardiac Anterior aorta Proventriculus Crop
DILP3	IPCs	IPCs Muscle cells of midgut	Corpora cardiac Anterior aorta Proventriculus Crop
DILP4	Anterior midgut	--------	---------
DILP5	IPCs Principle cells of renal tubules	IPCs Principle cells of renal tubules Follicle cells of ovary	Corpora cardiac Anterior aorta Proventriculus Crop

DILP6	Adipose cells Salivary Glands Heart Glial cells of CNS	Adipose cells	----------
DILP7	Abdominal neuromeres	Abdominal neuromeres	Brain neuropil Hindgut Reproductive tract
DILP8	Imaginal disc	Ovary	----------

Apdated from Nassel *et al., 2013*

In *Drosophila* insulin signaling pathway has been shown to lead to a reduction in body size and female sterility (Spradling,2001). Chico is an adaptor protein homologous to the vertebrate insulin receptor substrate(IRS) and controls cell proliferation, cell size, and overall body growth. Chico mutants flies are small in size, and homozygous mutant females are sterile have small ovaries. Their egg chambers fail to develop into the vitellogenic stages (stage 8 onwards; Bohni et al., 1999). Transplantation of *Chico* ovaries into wildtype females failed to rescue this defect indicating that insulin signaling is necessary for the egg chambers to undergo development beyond the vitellogenic stage (Richard *et al.,* 2005).

To test whether *dilp* levels are altered in *Dmon1*$^{\Delta 181}$ mutants, quantitative RT-PCR was done on RNA isolated form *Dmon1*$^{\Delta 181}$ mutants. We found that there is more than 50% decrease in transcript levels of *dilp*1,3,4,5 and 6 and an increase in the level of *dilp8*. *Dilps* 2 and 7 did not show any significant change (Figure3.6.1). This suggests that insulin signaling may be affected in *Dmon1*$^{\Delta 181}$ mutants.

Figure3.6.1

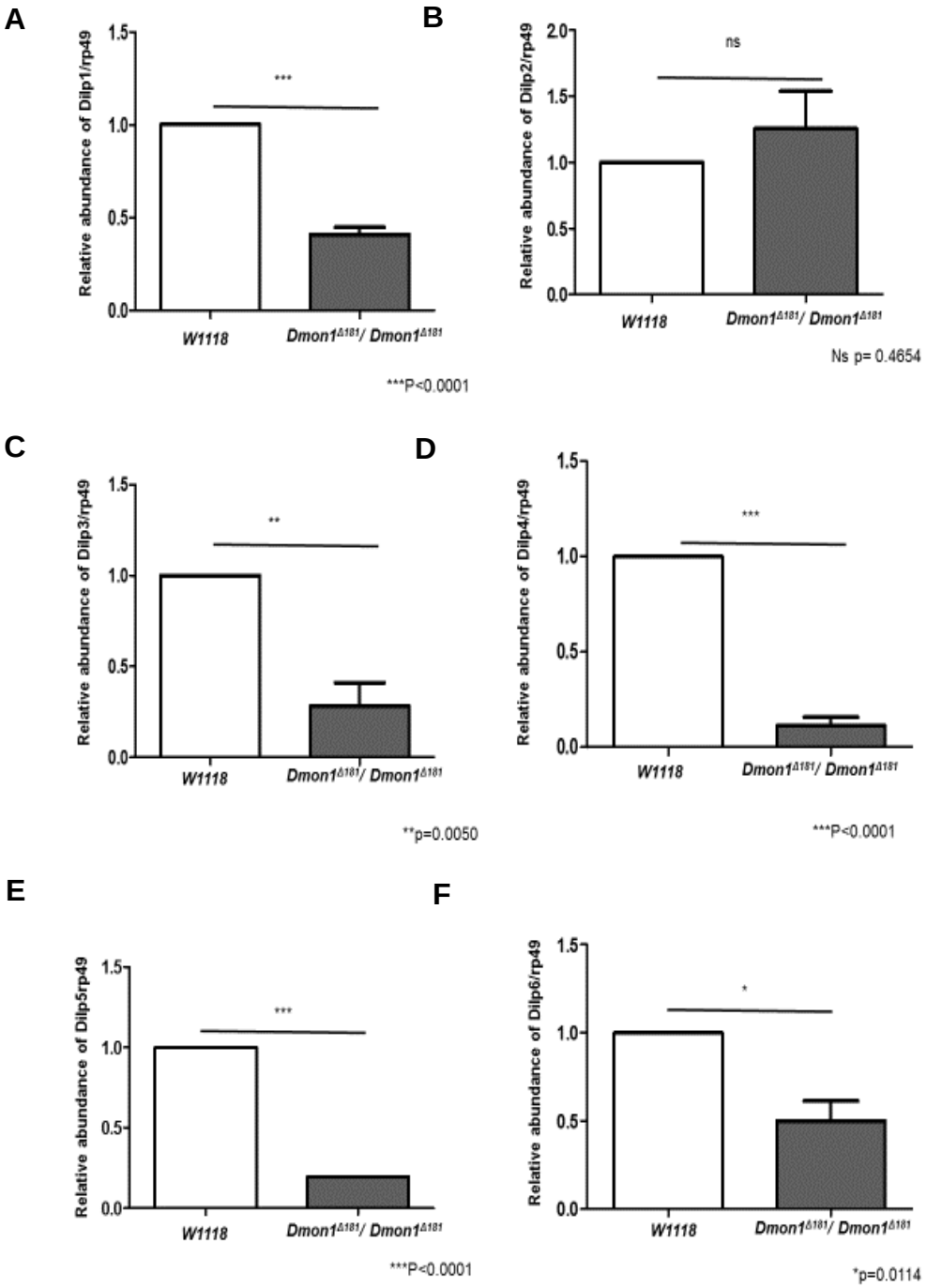
A
Relative abundance of Dilp1/rp49
1.5
1.0
0.5
0.0
***
W1118
Dmon1Δ181/ Dmon1Δ181
***P<0.0001
B
Relative abundance of Dilp2/rp49
2.0
1.5
1.0
0.5
0.0
ns
W1118
Dmon1Δ181/ Dmon1Δ181
Ns p= 0.4654
C
Relative abundance of Dilp3/rp49
1.5
1.0
0.5
0.0
**
W1118
Dmon1Δ181/ Dmon1Δ181
**p=0.0050
D
Relative abundance of Dilp4/rp49
1.5
1.0
0.5
0.0
***
W1118
Dmon1Δ181/ Dmon1Δ181
***P<0.0001
E
Relative abundance of Dilp5rp49
1.5
1.0
0.5
0.0
***
W1118
Dmon1Δ181/ Dmon1Δ181
***P<0.0001
F
Relative abundance of Dilp6/rp49
1.5
1.0
0.5
0.0
*
W1118
Dmon1Δ181/ Dmon1Δ181
*p=0.0114

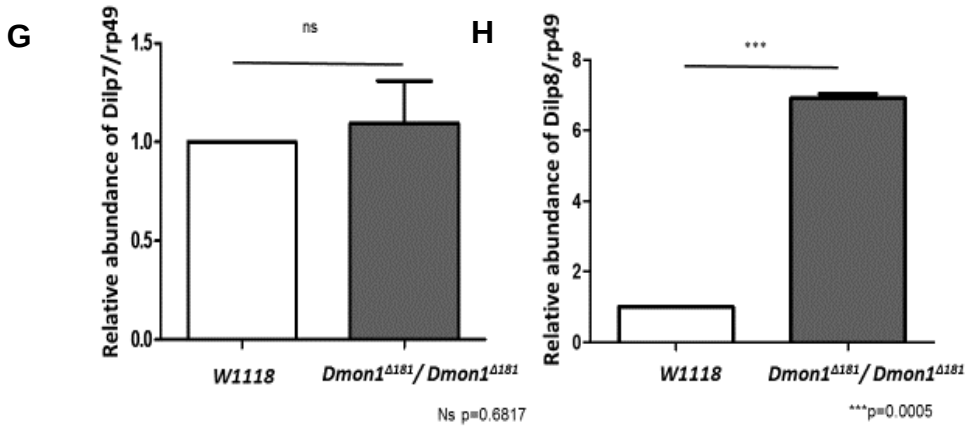

Figure3.6.1: Quantification of the levels of different *dilps* in *Dmon1$^{\Delta 181}$* mutant flies.
(A-H) Graph showing the abundance of Orb mRNA normalized to ribosomal protein transcript rp49. Significant change in the level of different dilps(1-8) in *Dmon1$^{\Delta 181}$/Dmon1$^{\Delta 181}$* mutant flies.

3.7. Insulin feeding partially rescues the *Dmon1$^{\Delta 181}$* ovary phenotype.

Because, of the decrease in *dilp* levels, we checked if feeding insulin to mutant adult flies would improve their viability and rescue the ovary phenotype. Homozygous *Dmon1$^{\Delta 181}$* exhibit a half-life of approximately 3 days; the animals fail to survive beyond 5 days. When *Dmon1$^{\Delta 181}$* mutants were kept on medium containing insulin at 5µg/ml, the animals survived for at least 10 days with a half-life of approximately 5-6 days. An equal number of adult mutants were kept in normal and insulin containing a medium. The ovaries of the control and insulin fed animals were dissected on the fifth day. In control, five-day-old *Dmon1$^{\Delta 181}$* mutants, the ovaries were very small. However, insulin fed flies of the same age showed near normal sized ovaries (Figure 3.7.1A to D). At day 10, these animals showed even more normal looking ovaries with Orb levels comparable to age-matched wildtype ovaries. (Figure 3.7.1E). Since most *Dmon1$^{\Delta 181}$* mutants die between day 5-7, we decided to quantitate the rescue in insulin fed flies at day 5. As shown in figure 3.7.1G & H, feeding insulin was able to rescue, at least partially, the 'stalling phenotype' observed in mutant ovarioles. Of the 40 ovarioles examined, 50 % showed late stage or vitellogenic egg chambers. Orb levels also seemed to be partially rescued at this time point. Based on these results we conclude that feeding insulin to *Dmon1$^{\Delta 181}$* mutants significantly rescues the ovary phenotype at day 5. A better rescue is observed at day 10. Despite the ovary rescue and a mild

improvement in lifespan (as the animals survive up to 10 days), we did not observe any rescue of the motor defects characteristic of *Dmon1*$^{\Delta 181}$ mutant.

Taken together, these results suggest that the ovary phenotype in *Dmon1*$^{\Delta 181}$ mutants is likely to be due to impaired insulin signaling caused by a decrease in expression or secretion of *dilps* by neurons and that Mon1 may function as an upstream regulator of insulin signaling.

Figure3.7.1

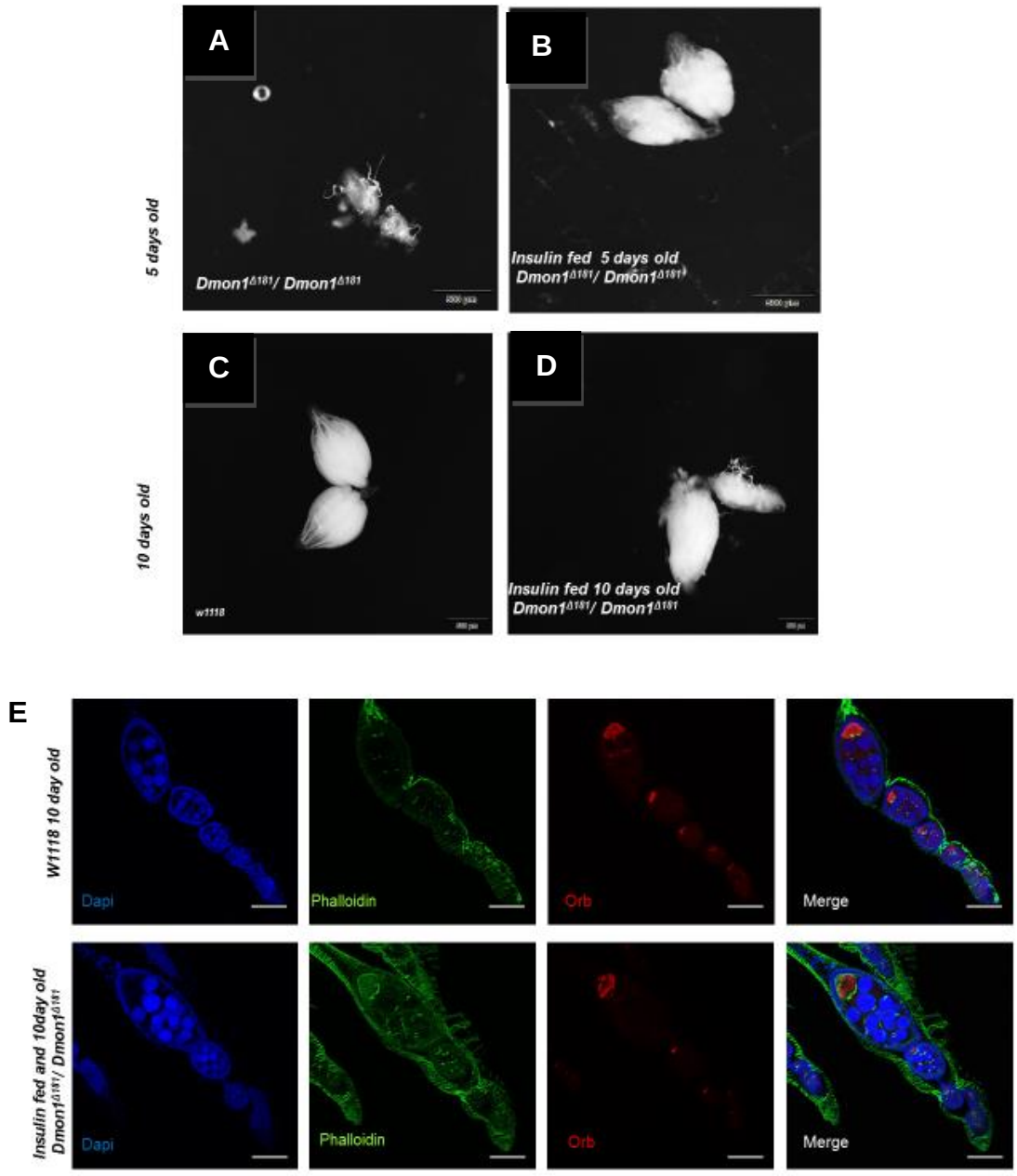

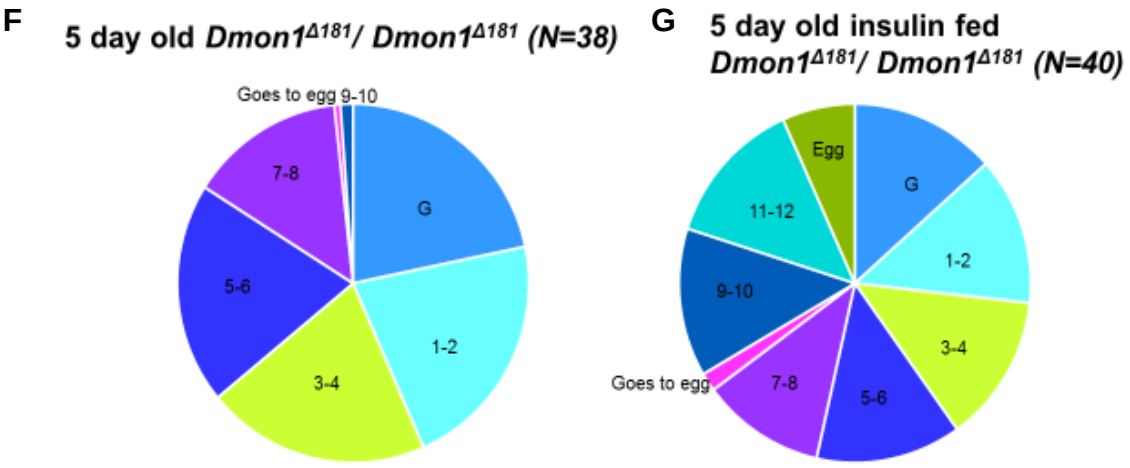

Figure3.7.1 Insulin feeding leads to a significant rescue of the *Dmon1$^{\Delta 181}$* ovary phenotype.

(A) Representative image of a 5 days old *Dmon1$^{\Delta 181}$/Dmon1$^{\Delta 181}$* ovaries.

(B) 5 days old insulin fed *Dmon1$^{\Delta 181}$/Dmon1$^{\Delta 181}$* ovaries.

(C) 10 days old wildtype ovaries.

(D) 10 days old insulin fed *Dmon1$^{\Delta 181}$/Dmon1$^{\Delta 181}$* ovaries.

(E) Representative image of a wildtype and 10day old insulin fed *Dmon1$^{\Delta 181}$/Dmon1$^{\Delta 181}$* ovariole showing egg chambers from germarium to stage 8. DAPI(blue) stained nuclei, phalloidin (green) stained actin and Orb expression is in red. Intensity of Orb in both wildtype and *Dmon1$^{\Delta 181}$/Dmon1$^{\Delta 181}$* seem to look same.

(F) Pie charts showing the distribution of the occurrence of the different stages of egg chambers in 5 day old *Dmon1$^{\Delta 181}$/Dmon1$^{\Delta 181}$* show stalling of egg chambers at stages 7-8. Very few ovarioles show presence of egg chambers older than stage 8.

(G) 5 day old insulin fed *Dmon1$^{\Delta 181}$/Dmon1$^{\Delta 181}$* late stages and egg formation is seen. 50% ovarioles show egg formation

3.8. Protein purification for antibody generation.

To understand the cellular and sub-cellular localization of Mon1 we need to develop reagents to visualize endogenous Mon1. Antibodies are useful reagents to study expression pattern and biochemistry of molecules. In order to generate an antibody against Mon1, I have standardized the expression and purification of the Mon1 protein. Mon1 had been cloned into the pGEX vector in frame with the N-terminal GST tag. To test expression of this clone, a pilot scale induction was carried out using 1mM IPTG. A strongly induced band corresponding to the fusion protein was observed at 86kD.To confirm that this was indeed the fusion protein, a small scale purification was done using glutathione beads. Shown in figure3.8.1C is the affinity purified protein.

Based on the pilot experiment, a large scale expression and purification were attempted. However, after affinity binding to GST beads, we were able to elute only 40-50% of the total protein using thrombin cleavage of the GST tag. Different conditions were used to optimize cleavage as shown in Figure 3.8.1D-E. Troubleshooting was undertaken to increase the yield of purified, cleaved Mon1 by using 0.1% Triton X-100, 1% Triton X-100 with 0.5mM DTT, by varying the pH of phosphate-citrate buffer used to elute the protein that remained stuck to the beads, thrombin cleavage at room temperature for 3 hours and using 8M urea at room temperature and separately at 37 degrees for half an hour ((Figure 3.8.1D-J). None of these methods worked efficiently. We chose, therefore, to sub-clone Mon1 into pET vector with N terminal His tag, to circumvent the problem caused by GST. Attempts will be made to purify His-Mon1 to generate an antibody for the same.

Figure3.8.1

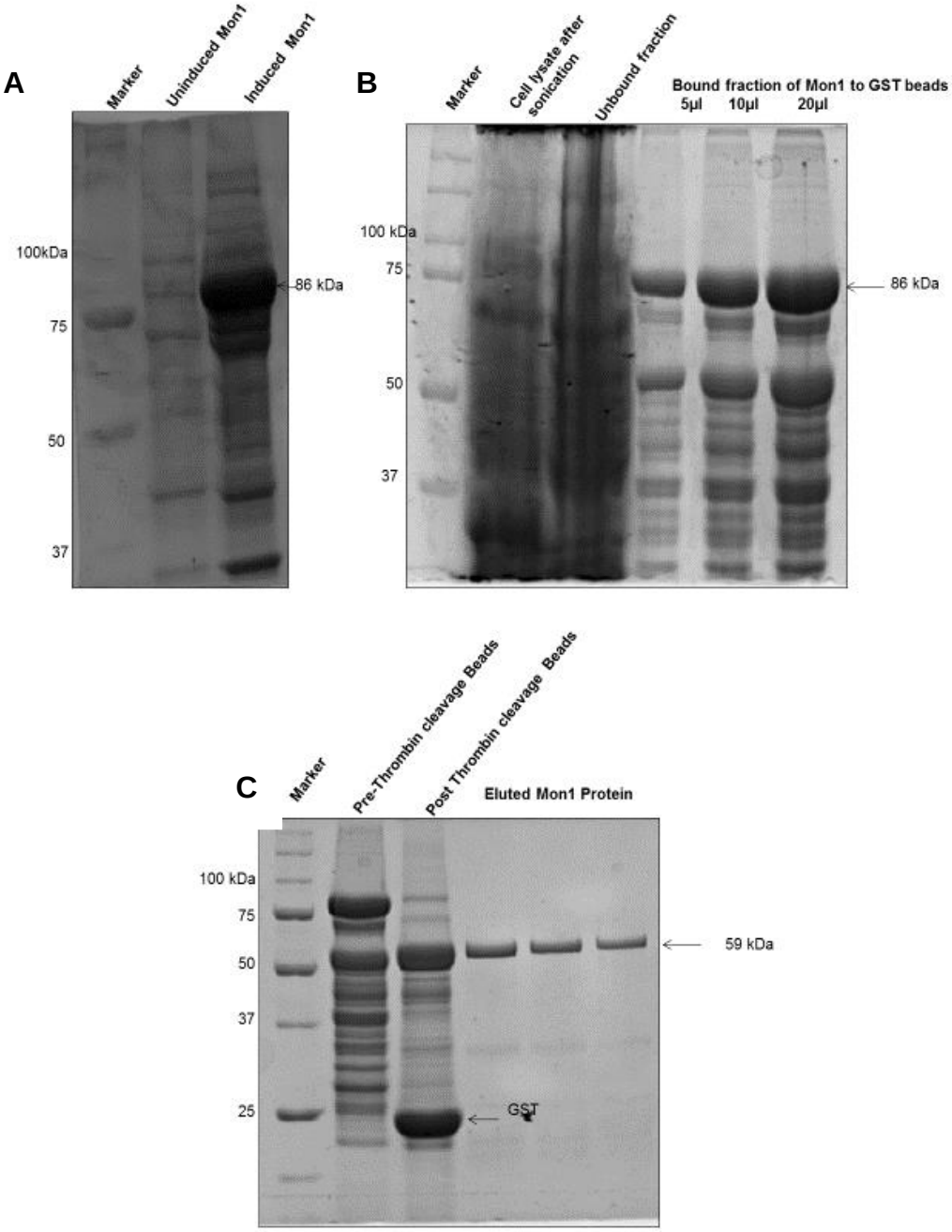

Figure3.8.1: Protein expression and purification

(A) SDS page gel stained with coomassie blue to demonstrate the expression of GST-Mon1 in BL21(DE3) cells induced with 1mM IPTG at 25degrees for 6 hrs. Lysate was loaded on to the gel. The molecular weight of Mon1 is 60kDa and GST is 26kDa.

(B) SDS page gel stained with coomassie blue to demonstrate the pulldown efficiency of Mon1 using GST beads, in comparison with lysate after sonication and unbound fraction after pulldown.

(C) Thrombin cleavage of GST-Mon1 to cleave the GST tag of fusion protein to obtain purified protein.

D

Treatment with 0.1% TritonX

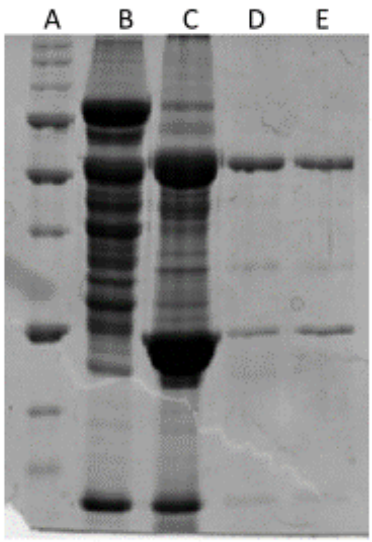

A – Marker
B - Pre thrombin cleavage beads
C - Beads after washing with 0.1% triton X
D – Elute 1
E – Elute 2

E

1% Triton X and 0.5mM DTT

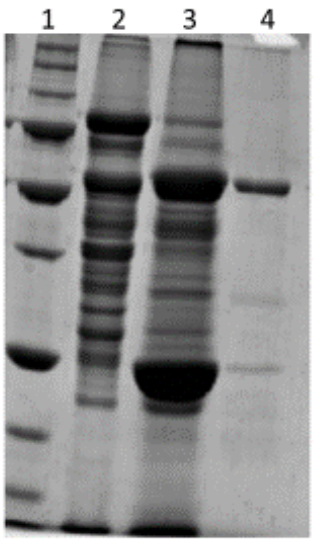

1 – Marker
2 - Pre thrombin cleavage beads
3 - Beads after washing with 1% triton X and 0.5mM DTT
4 – Elute

F

Different pH phosphate citrate buffer

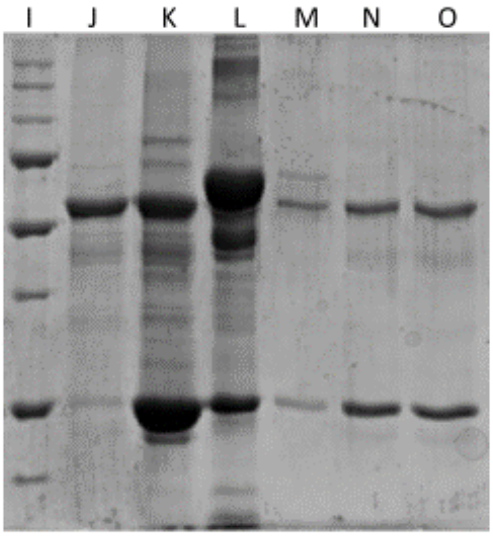

I – Marker
J – Elute of stored beads in 1x TBS for 2 days
K - Beads loading without any treatment
L - Elute with 2.6pH phosphate citrate buffer
M – Elute with 4.6pH
N – Elute with 5.6pH
O – Elute with 7pH

G

pH2.6 phosphate citrate buffer

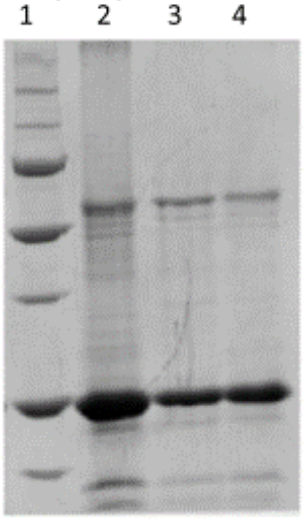

A – Marker
B - Beads after treatment
C -Elute 1
D – Elute 2

H

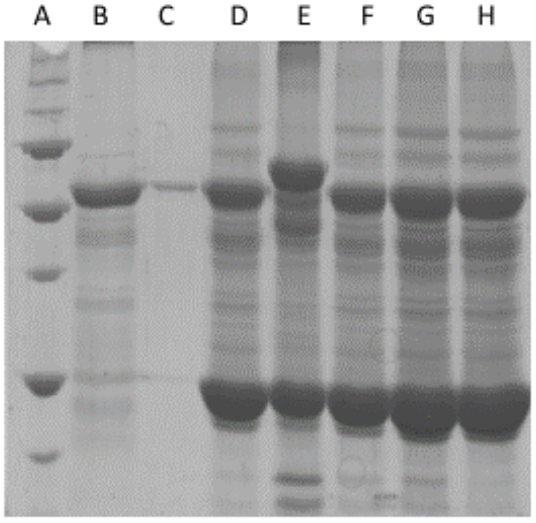

A – Marker
B – Elute of stored beads in 1x TBS for 2 days
C - Elute of beads in 0.1x TBS
D – Beads before treatment
E – Beads after treated 2.6pH phosphate citrate buffer
F – Beads after treated with 4.6pH
G – Beads after treated with 5.6pH
H – Beads after treated with 7pH

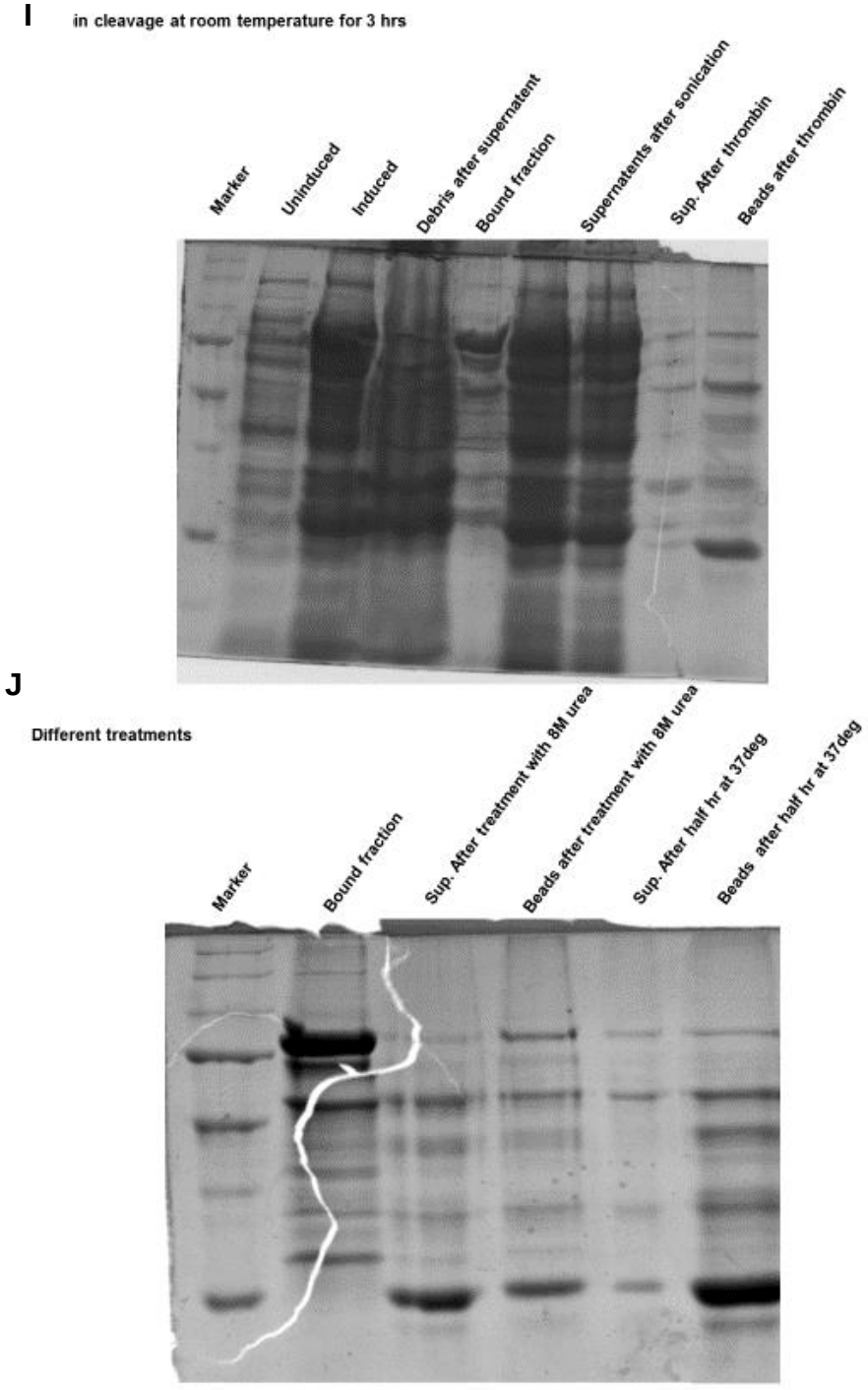

Figure3.8.2:Troubleshooting was undertaken to increase the yield of purified, cleaved Mon1

(D) using 0.1% Triton X-100

(E) 1% Triton X-100 with 0.5mM DTT,

(F-H) by varying the pH of phosphate citrate buffer used to elute the protein that remain stuck to the beads.

(I) thrombin cleavage at room temperature for 3 hours.

(J) using 8M urea at room temperature and separately at 37 degrees for half an hour.

4. Discussion

In this study, we have tried to understand the role of *Dmon1* during the development of the ovary. *Dmon1* mutants are sterile and show the presence of extremely small ovaries with fewer ovarioles. The latter seen in at least two allelic mutants of *Dmon1*. Each ovariole shows the presence of small egg chambers stage most of which appear to be stalled in the previtellogenic stage. Very few ovarioles showed egg chambers at the the vitellogenic stage (stage 8 onwards) and having mature eggs. In addition, the egg chambers showed a decrease in *orb* levels in the oocyte and 10-14% degeneration of vitellogenic egg chambers. Interestingly, expression of *Dmon1* pan-neuronally or in octopaminergic neurons alone was sufficient to rescue all the phenotypes associated with ovaries. Further loss of Dmon1 in neurons rather than the germline was found to be responsible for the small ovary phenotype suggesting a non-cell autonomous control by *Dmon1*.

Insulin signaling is a conserved pathway central to growth and metabolism. Mutations in insulin substrate protein (*Chico*), the ortholog of vertebrate IRS-4 (Bohini *et al.,*1999) results in sterility with egg chambers that are unable enter the vitellogenic stage. Insulin signaling is thus necessary for the maintenance of the vitellogenesis in *Drosophila* (Spradling *et al.,*2001; Richard *et al.,*2005). We find that expression of *dilps* 1,3,5, 6 are significantly reduced (more than 50%) in $Dmon1^{\Delta 181}$ mutants, and feeding of insulin to homozygous $Dmon1^{\Delta 181}$ females rescues the ovary phenotypes including ovariole number suggesting that insulin signaling is probably affected in *Dmon1* mutants.

Expression of *Dmon1* in octopaminergic neurons is sufficient to rescue both lethality and the sterility phenotype in the mutants. The fact that loss of *Dmon1* in the germline does not give rise to the small ovary phenotype strongly supports a neural basis for this defect. Octopaminergic neurons are known to control and modulate many behaviors in *Drosophila* (Luo et al., 2014). The terminals of some of these neurons lie in close proximity to the insulin-producing cells (IPCs) which secrete Dilps 2, 3 and 5. Moreover, IPCs are known to express OAMB octopaminergic receptors on their surface indicating that they are responsive to octopamine. Since feeding insulin to Dmon1 mutants can rescue the ovary phenotype, it suggests that DMon1 in

octopaminergic neurons is necessary for the synthesis and/or secretion of Dilps. This will need to be confirmed by examining the transcript levels of dilps in 'rescue' animals.

Our data suggests that transcript levels of *dilp 3* and 5 but not *dilp2*, are lowered. This indicates that loss of DMon1 affects the transcription of these genes. Whether the circulating levels of Dilps is also affected needs to be determined. It is possible that even though Dilp2 mRNA levels are unaltered, the expression and release of this protein may be affected. Supporting this, we find that expression of Dilp2 in Dilp2 neurons is not sufficient to rescue the lethality and ovary phenotype in *Dmon1*$^{\Delta 181}$ mutants (data not shown). This needs to be tested by checking for the amount of this protein in the hemolymph. Nevertheless, our results suggest Dmon1 be genetically upstream of insulin signaling.

How does DMon1 regulate Dilp expression? In the neuromuscular junction, *Dmon1* appears to be secreted by the presynaptic terminal (Deivasigamani et al., 2015) suggesting that it can function in a non-cell autonomous manner. We checked if *DMon1* is secreted into the hemolymph by expressing the tagged *DMon1* in neurons. However, we did not obtain any clear results to support the presence of DMon1 in the hemolymph.

As seen at the neuromuscular junction, it is possible that *Dmon1* functions in a similar manner to regulate expression of OAMB thus affecting the activation of IPCs. Another possibility is that *Dmon1* may also function to facilitate the release of certain factors that influence the expression of Dilps. These possibilities need to be explored by checking for expression of OAMB receptors and Dilps in the IPCs.

Secretion of Dilps is also regulated by ecdysone and juvenile hormone. Preliminary results of feeding *Dmon1*$^{\Delta 181}$ mutant flies with 20-OH ecdysone did not seem to rescue the ovary phenotype suggesting that this pathway may not be involved.

The observation that feeding of human insulin to *Dmon1*$^{\Delta 181}$ mutant flies rescues the ovary phenotype strongly suggests that these ovary defects are due to impaired insulin signalling. The extent of rescue can be correlated to the amount of insulin intake based on the extent of rescue seen in 5 days and 10 day old mutants fed on insulin containing a medium. We find that mutant flies fed on insulin medium for 10 days, show a near complete rescue of the ovary phenotypes including the rescue of the ovariole number, orb levels, and presence of eggs. A similar rescue is seen at day 5 although these

ovaries tend to have a few ‘mutant-like’ ovarioles. At both time points, we do not see any suppression of the degeneration phenotype suggesting that it might be independent of insulin signaling.

In summary, we conclude that *Dmon1* is necessary for ovary development and it does this by regulating the insulin pathway. The challenge for the future study is to understand the mechanism of crosstalk between Mon1 and insulin pathway and identification of the neural circuit involved in this process.

5. References

Bower, D.V., Lee, H.K., Lansford, R., Zinn, K., Warburton, D., Fraser, S.E., and Jesudason, E.C. (2014). Airway branching has conserved needs for local parasympathetic innervation but not neurotransmission. BMC Biology *12*, 92.

Brogiolo, W., Stocker, H., Ikeya, T., Rintelen, F., Fernandez, R., and Hafen, E. (2001). An evolutionarily conserved function of the *Drosophila* insulin receptor and insulin-like peptides in growth control. Current Biology: *11*, 213-221.

Cao, C., and Brown, M.R. (2001). Localization of an insulin-like peptide in brains of two flies. Cell and Tissue research *304*, 317-321.

Cui, Y., Zhao, Q., Gao, C., Ding, Y., Zeng, Y., Ueda, T., Nakano, A., and Jiang, L. (2014). Activation of the Rab7 GTPase by the MON1-CCZ1 Complex Is Essential for PVC-to-Vacuole Trafficking and Plant Growth in Arabidopsis. The Plant cell *26*, 2080-2097.

Cui, Y., Zhao, Q., Xie, H.T., Wong, W.S., Wang, X., Gao, C., Ding, Y., Tan, Y., Ueda, T., Zhang, Y.*, et al.* (2017). MONENSIN SENSITIVITY1 (MON1)/CALCIUM CAFFEINE ZINC SENSITIVITY1 (CCZ1)-Mediated Rab7 Activation Regulates Tapetal Programmed Cell Death and Pollen Development. Plant Physiology *173*, 206-218.

Deivasigamani, S., Basargekar, A., Shweta, K., Sonavane, P., Ratnaparkhi, G.S., and Ratnaparkhi, A. (2015). A Presynaptic Regulatory System Acts Transsynaptically via Mon1 to Regulate Glutamate Receptor Levels in *Drosophila*. *Genetics 201*, 651-664.

Drummond-Barbosa, D., and Spradling, A.C. (2001). Stem cells and their progeny respond to nutritional changes during *Drosophila* oogenesis. Developmental biology *231*, 265-278.

Eliazer, S., and Buszczak, M. (2011). Finding a niche: studies from the *Drosophila* ovary. Stem cell research & therapy *2*, 45.

Enell, L.E., Kapan, N., Soderberg, J.A., Kahsai, L., and Nassel, D.R. (2010). Insulin signaling, lifespan and stress resistance are modulated by metabotropic GABA receptors on insulin-producing cells in the brain of *Drosophila*. PloS one *5*, e15780.

Frydman, H.M., and Spradling, A.C. (2001). The receptor-like tyrosine phosphatase lar is required for epithelial planar polarity and for axis determination within *Drosophila* ovarian follicles. Development *128*, 3209-3220.

Harris, L.K., Crocker, I.P., Baker, P.N., Aplin, J.D., and Westwood, M. (2011). IGF2 actions on trophoblast in human placenta are regulated by the insulin-like growth factor 2 receptor, which can function as both a signaling and clearance receptor. Biology of reproduction *84*, 440-446.

Hegedus, K., Takats, S., Boda, A., Jipa, A., Nagy, P., Varga, K., Kovacs, A.L., and Juhasz, G. (2016). The Ccz1-Mon1-Rab7 module and Rab5 control distinct steps of

autophagy. Molecular Biology of the cell *27*, 3132-3142.

Huynh, J.R., and St Johnston, D. (2000). The role of BicD, Egl, Orb and the microtubules in the restriction of meiosis to the *Drosophila* oocyte. Development *127*, 2785-2794.

Ikeya, T., Galic, M., Belawat, P., Nairz, K., and Hafen, E. (2002). Nutrient-dependent expression of insulin-like peptides from neuroendocrine cells in the CNS contributes to growth regulation in *Drosophila*. Current Biology *12*, 1293-1300.

Knox, S.M., Lombaert, I.M., Haddox, C.L., Abrams, S.R., Cotrim, A., Wilson, A.J., and Hoffman, M.P. (2013). Parasympathetic stimulation improves epithelial organ regeneration. Nature Communications *4*, 1494.

Kumar, A., and Brockes, J.P. (2012). Nerve dependence in tissue, organ, and appendage regeneration. Trends in Neurosciences *35*, 691-699.

Lantz, V., Chang, J.S., Horabin, J.I., Bopp, D., and Schedl, P. (1994). The *Drosophila* orb RNA-binding protein is required for the formation of the egg chamber and establishment of polarity. Genes & development *8*, 598-613.

Lee, K.S., You, K.H., Choo, J.K., Han, Y.M., and Yu, K. (2004). *Drosophila* short neuropeptide F regulates food intake and body size. The Journal of biological chemistry *279*, 50781-50789.

Luo, J., Lushchak, O.V., Goergen, P., Williams, M.J., and Nassel, D.R. (2014). *Drosophila* insulin-producing cells are differentially modulated by serotonin and octopamine receptors and affect social behavior. PloS one *9*, e99732.

Makhijani, K., Alexander, B., Tanaka, T., Rulifson, E., and Bruckner, K. (2011). The peripheral nervous system supports blood cell homing and survival in the *Drosophila* larva. Development *138*, 5379-5391.

Nassel, D.R., Kubrak, O.I., Liu, Y., Luo, J., and Lushchak, O.V. (2013). Factors that regulate insulin-producing cells and their output in *Drosophila*. Frontiers in Physiology *4*, 252.

Polupanov, A.S., Nazarko, V.Y., and Sibirny, A.A. (2011). CCZ1, MON1, and YPT7 genes are involved in pexophagy, the Cvt pathway and non-specific macroautophagy in the methylotrophic yeast Pichia pastoris. Cell biology international *35*, 311-319.

Poteryaev, D., Datta, S., Ackema, K., Zerial, M., and Spang, A. (2010). Identification of the switch in early-to-late endosome transition. Cell *141*, 497-508.

Richard, D.S., Rybczynski, R., Wilson, T.G., Wang, Y., Wayne, M.L., Zhou, Y., Partridge, L., and Harshman, L.G. (2005). Insulin signaling is necessary for vitellogenesis in *Drosophila* melanogaster independent of the roles of juvenile hormone and ecdysteroids: female sterility of the chico1 insulin signaling mutation is autonomous to the ovary. Journal of Insect Physiology *51*, 455-464.

Wang, C.W., Stromhaug, P.E., Shima, J., and Klionsky, D.J. (2002). The Ccz1-Mon1 protein complex is required for the late step of multiple vacuole delivery pathways. The

Journal of Biological Chemistry *277*, 47917-47927.